



# Optimalizace konstrukce motoru lodi

## Diplomová práce

*Studijní program:* N2301 – Strojní inženýrství

*Studijní obor:* 2302T010 – Strojirentsvi

*Autor práce:* **Fernando Rafael Rubio Burga**

*Vedoucí práce:* prof. Ing. Tomáš Vít, Ph.D.





# Optimization of the boat engine design

## Master thesis

*Study programme:* N2301 – Mechanical Engineering  
*Study branch:* 2302T010 – Machines and Equipment design

*Author:* **Fernando Rafael Rubio Burga**  
*Supervisor:* prof. Ing. Tomáš Vít, Ph.D.





## Zadání diplomové práce

# Optimization of the boat engine design

*Jméno a příjmení:* **Fernando Rafael Rubio Burga**  
*Osobní číslo:* S18000191  
*Studijní program:* N2301 Mechanical Engineering  
*Studijní obor:* Machines and Equipment Design  
*Zadávací katedra:* Katedra energetických zařízení  
*Akademický rok:* 2019/2020

### Zásady pro vypracování:

Machine shape optimization using the CFD analysis is currently a widely used tool for improving the parameters of the machines. The subject of this work is the investigation of the influence of shape change on the boat engine parameters (flow, thrust, efficiency). The scaled model of the boat engine will be investigated. The main tool for the investigation will be the CFD computations. Validation of the CFD results should be done by the comparison with experimental data.

The thesis contains:

1. Description of the boat engine including the main parameters.
2. Review of the CFD and experimental methods.
3. Description of the physical and material models used for CFD simulations.
4. CFD simulation of the flow inside the boat engine.
5. Comparison of the experimental and CFD results.
6. Evaluation and discussion of results.

Rozsah grafických prací:  
Rozsah pracovní zprávy:  
Forma zpracování práce:  
Jazyk práce:

60  
tištěná/elektronická  
Angličtina



### Seznam odborné literatury:

FERZIGER, Joel H. a Milovan PERIĆ. Computational methods for fluid dynamics. 3., rev. ed. Berlin: Springer, 2002. ISBN 3-540-42074-6.

WHITE, Frank M. Fluid mechanics. Eighth edition in SI units. New York: McGraw Hill Education, [2016]. ISBN 978-981-4720-17-5.

Additional literature will be set after the consultation with students.

Vedoucí práce: prof. Ing. Tomáš Vít, Ph.D.  
Katedra energetických zařízení

Datum zadání práce: 1. listopadu 2019  
Předpokládaný termín odevzdání: 30. dubna 2021

prof. Dr. Ing. Petr Lenfeld  
děkan



doc. Ing. Petra Dančová, Ph.D.  
vedoucí katedry

V Liberci dne 14. února 2020

## Declaration

I hereby certify, I, myself, have written my master thesis as an original and primary work using the literature listed below and consulting it with my thesis supervisor and my thesis counsellor.

I acknowledge that my bachelor master thesis is fully governed by Act No. 121/2000 Coll., the Copyright Act, in particular Article 60 – School Work.

I acknowledge that the Technical University of Liberec does not infringe my copyrights by using my master thesis for internal purposes of the Technical University of Liberec.

I am aware of my obligation to inform the Technical University of Liberec on having used or granted license to use the results of my master thesis; in such a case the Technical University of Liberec may require reimbursement of the costs incurred for creating the result up to their actual amount.

At the same time, I honestly declare that the text of the printed version of my master thesis is identical with the text of the electronic version uploaded into the IS/STAG.

I acknowledge that the Technical University of Liberec will make my master thesis public in accordance with paragraph 47b of Act No. 111/1998 Coll., on Higher Education Institutions and on Amendment to Other Acts (the Higher Education Act), as amended.

I am aware of the consequences which may under the Higher Education Act result from a breach of this declaration.



June 11, 2020

Fernando Rafael Rubio Burga

## Acknowledgements

I wish to thank all the people whose assistance was a milestone in the completion of this project, professors, family, the TUL, and special thanks to the Ministry of Education, Youth and Sports of the Czech republic, for giving me the opportunity to study here and grow as a person.

## Abstract

Electric vehicles gain more importance due to environment protection policies as well as the technology of electric motors and batteries are in constant improvement. Some countries and companies are developing electric water crafts where usages could be military, transportation as well as private high speed and high efficiency vehicles. Progressive adoption of the water jet pump is achieved as cheaper materials are available on the market and the technology makes more affordable to implement these high speed propellers for water crafts. Materials must be taken into account in order to prevent corrosion, as well as the water jet pump must be designed according to a high efficiency electric motor as to minimize problems such as cavitation for maximum durability of the pump. In this thesis, designing a water jet pump for watercraft powered by an electric motor configure making a step forward on high quality electric vehicles design.

**Keywords:** water jet, pump jet, electric vehicles, watercraft

# Contents

List of Symbols . . . . .	13
<b>1 Description of the boat engine including the main parameters</b>	<b>15</b>
1.1 State of the art of boats . . . . .	15
1.2 The centrifugal pump . . . . .	16
1.3 Pump Theory . . . . .	17
1.3.1 Head Coefficient . . . . .	17
1.3.2 Specific Flow - Flow Coefficient . . . . .	18
1.3.3 Specific Speed . . . . .	18
1.3.4 Net Positive Suction Head (NPSH) . . . . .	18
1.3.5 Cavitation Coefficient . . . . .	18
1.3.6 Machine Reynolds Number . . . . .	19
1.3.7 Classification of impellers of working machines . . . . .	19
1.3.8 Characteristics of pump . . . . .	20
1.4 The Pump-Jet impeller . . . . .	20
1.4.1 General mechanism of jet pump operation . . . . .	22
1.4.2 Parameters affecting the pump-jet . . . . .	23
1.4.3 System decomposition . . . . .	24
1.4.4 Water jet configuration cases . . . . .	25
1.4.5 Pump jet design process . . . . .	25
1.5 Water jet equations . . . . .	26
1.5.1 Efficiency of a propulsor . . . . .	26
1.5.2 Power input to system . . . . .	27
1.5.3 Overall efficiency . . . . .	28
1.5.4 Nozzle velocity ratio (NVR) . . . . .	28
1.5.5 Thrust load coefficient . . . . .	28
1.5.6 Ideal jet efficiency . . . . .	28

1.5.7	Effective jet system . . . . .	28
1.5.8	Effective jet system in operation conditions . . . . .	29
1.5.9	Model net thrust . . . . .	29
1.5.10	Momentum velocity coefficient . . . . .	29
1.6	Thrust Vectored Control(TVC) . . . . .	29
1.7	Electrical Motor Theory . . . . .	29
1.7.1	Brushless Direct-Current Motors(BLDC) . . . . .	30
1.7.2	The Electric Speed Controller[10] . . . . .	31
<b>2</b>	<b>CFD methods</b>	<b>33</b>
2.1	Theory . . . . .	33
2.1.1	Pre-processing . . . . .	33
2.1.2	Processing . . . . .	36
2.1.3	Post-processing . . . . .	37
2.2	Specification of the problems . . . . .	37
2.2.1	Flow . . . . .	37
2.2.2	System . . . . .	37
2.3	Solution . . . . .	38
2.3.1	Flow . . . . .	38
2.3.2	System . . . . .	38
2.3.3	Computational mesh . . . . .	38
2.3.4	Convergence . . . . .	38
2.3.5	Post-processing . . . . .	38
<b>3</b>	<b>Software</b>	<b>39</b>
3.1	ANSYS . . . . .	39
3.2	MATLAB . . . . .	39
3.3	GNU Octave . . . . .	40
<b>4</b>	<b>Experimental methods</b>	<b>41</b>
4.1	Thrust measurement with load cell . . . . .	41
4.2	Power measurement . . . . .	41
4.3	Microcontroller Unit (MCU) . . . . .	43
<b>5</b>	<b>Results</b>	<b>46</b>
5.1	First Approach . . . . .	46

5.1.1	Electric motor . . . . .	46
5.1.2	Model dimension measurement . . . . .	47
5.1.3	Comparison between model and proposed design . . . . .	47
5.2	CFD Analysis . . . . .	54
5.2.1	System assumptions . . . . .	54
5.2.2	CAD Modelling and designs . . . . .	54
5.2.3	Meshing . . . . .	54
5.2.4	Boundary Conditions . . . . .	55
5.2.5	Design points . . . . .	55
5.3	Experimental Analysis . . . . .	56
<b>6</b>	<b>Results</b>	<b>58</b>
6.1	Conclusion . . . . .	62
	<b>Literature</b>	<b>64</b>
	<b>Attachments</b>	<b>A1</b>

## List of Figures

1.1	Li-Ion pricing and energy density 1991-2005. . . . .	16
1.2	Velocity diagram and velocity triangles at centrifugal pump. . . . .	17
1.3	NPSH in a blade . . . . .	19
1.4	Classification of impellers working machines . . . . .	20
1.5	Efficiency of pumps versus specific speed . . . . .	21
1.6	Performance curve of a pump . . . . .	22
1.7	Dimensionless performance graph of a pump, relating the head coefficient and the flow coefficient . . . . .	23
1.8	System decomposition, usage of the pump jet in a boat . . . . .	24
1.9	A small scale prototype of the water-jet pump to be placed inside the boat. . . . .	24
1.10	Water jet configuration case 1 . . . . .	26
1.11	Water jet configuration case 2 . . . . .	26
1.12	Water jet configuration case 3 . . . . .	27
1.13	Design process of a water jet pump, based on the Rolls-Royce standard . . . . .	27
1.14	Brushless motor selected BoatWing 3650KV . . . . .	31
1.15	Flycolor ESC A-SW090006 for 90A . . . . .	32
2.1	Mesh example . . . . .	37
4.1	HX711[22] . . . . .	42
4.2	Load cell picture . . . . .	42
4.3	Load cell drawing . . . . .	43
4.4	Electric current sensor ACS758[23] . . . . .	44
5.1	Electric Motor Calculation . . . . .	47
5.2	Water-Jet model in CAD . . . . .	47
5.3	Water-Jet Calculation, pump approach and cavitation analysis . . . . .	48

5.4	Water-Jet Calculations . . . . .	49
5.5	Water-Jet version 0 calculations . . . . .	50
5.6	Water-Jet version 0 Calculation, pump approach and cavitation analysis	51
5.7	Water Jet calculation blade step-diameter relation . . . . .	52
5.8	Water jet calculation performance comparison by size . . . . .	53
5.9	Water-Jet calculations by size . . . . .	53
5.10	CFD experiment with tank . . . . .	56
5.11	Experiment sketch . . . . .	57
5.12	Experiment wiring sketch . . . . .	57
6.1	Numerical results of the old model . . . . .	58
6.2	Numerical results of the proposed models . . . . .	59
6.3	Velocity results at the proposed models . . . . .	59
6.4	Comparison between experimental and theoretical velocity, mass flow rate, thrust and power of the old model @7m/s . . . . .	60
6.5	Comparison between experimental and theoretical velocity, mass flow rate, thrust and power of the model V0 @7m/s . . . . .	61

## List of Symbols

$\beta_1$	Angle of relative velocity in inlet	[1]
$\beta_2$	Angle of relative velocity in outlet	[1]
$\Omega$	Angular frequency	[1]
$\rho$	Density	$[kg \cdot m^{-3}]$
$n_b$	Dimensionless speed revolution	[1]
$I$	Electric current	$[A]$
$P_{JSE0}$	Effective jet system power	$[W]$
$P_{JSE}$	Effective jet system power in operational conditions	$[W]$
$n$	Efficiency of a propulsor	[1]
$p_{outeff}$	Effective power delivered by system	$[W]$
$Q$	Flow rate	$[m^3 \cdot s^{-1}]$
$n_0$	Free stream efficiency	[1]
$U_{wjx}$	Flow velocity at point x	$[m \cdot s^{-1}]$
$U_{exn}$	Flow velocity of exhaust	$[m \cdot s^{-1}]$
$Q_{wj}$	Flow rate of waterjet	$[m^3 \cdot s^{-1}]$
$g$	Gravity acceleration	$9.80665 [m \cdot s^{-2}]$ (exact)
$\psi$	Head coefficient	[1]
$d_1$	Inner diameter of wheel	$[m]$
$b_1$	Input edge of wheel	$[m]$
$U_1$	Input impeller blade speed	$[m \cdot s^{-1}]$
$V_1$	Input absolute velocity	$[m \cdot s^{-1}]$
$W_1$	Input relative velocity	$[m \cdot s^{-1}]$
$r_1$	Input impeller radius	$[m]$
$p_{in}$	Inlet pressure	$[Pa]$
$n_{int}$	Interaction efficiency	[1]
$n_i$	Ideal Jet efficiency	[1]
$\Delta M_x$	Model net thrust	$[N]$
$c_{mx}$	Momentum velocity coefficient x	[1]
$NPSH$	Net positive suction head	$[m]$
$A_n$	Nozzle area	$[m^2]$
$NVR$	Nozzle velocity ratio	[1]
$\theta_N$	Nozzle angle	[1]
$E_x$	Power at point x	$[W]$

$T$  Thrust [ $N$ ]  
 $K_t$  Torque constant for electric motors [ $N \cdot m \cdot A^{-1}$ ]  
 $d_2$  Outer diameter of wheel [ $m$ ]  
 $U_2$  Output impeller blade speed [ $m \cdot s^{-1}$ ]  
 $V_2$  Output absolute velocity [ $m \cdot s^{-1}$ ]  
 $W_2$  Output relative velocity [ $m \cdot s^{-1}$ ]  
 $r_2$  Output impeller radius [ $m$ ]  
 $n_d$  Overall efficiency [1]  
 $b_2$  Output edge of wheel [ $m$ ]  
 $\Delta P$  Pressure Head of pump [ $m$ ]  
 $P_{in}$  Power input to system [ $W$ ]  
 $P_{loss}$  Power losses [ $W$ ]  
 $\Omega_s$  Specific Speed [1]  
 $\Omega_{ss}$  Suction Specific Speed [1]  
 $C_{TN}$  Thrust load coefficient [1]  
 $T_{net}$  Thrust net [ $N$ ]  
 $T_{jet}$  Thrust jet [ $N$ ]  
 $p_v$  Vapor pressure [ $Pa$ ]  
 $\phi$  Volume rate coefficient [1]

# 1 Description of the boat engine including the main parameters

## 1.1 State of the art of boats

Electric Boats are in an economic boom with more than two digits growth per year in market according to the Advanced Market Analytic [1] and many companies starting to produce these vehicles as well as fund raising. The approach comes from hybrid boats to fully electric ones, in the case of Sweden the country is preparing to fully replace their ferry car boats to electric ones by 2045, this year 2019 they are preparing to release they 100m hybrid car ferry capable of carrying 300 passengers and 80 cars by the company Danfoss Editron, the boat stores energy in its 949kWh batteries[2] . Electric motors have many advantages against diesel ones, they have fewer parts, can be operating for years without any maintenance required, high quality electric motors have constant torque across all the range of speed operation, due to torque is depending on the following equation:

$$T/I = K_t \tag{1.1}$$

where  $T$  is the torque of the electric motor and  $I$  is the current that flows through the motor wires. The relation of the two of them is a constant  $K_t$  called torque constant which is property of the motor itself, therefore at constant current flow, the torque is also constant. This is significant advantage against every other engine. Across time electric vehicles are replacing internal combustion ones, as the price drops down the energy density of them is growing, as companies are investing in lithium factories. In 1.1, it can be seen more clearly the relationship between price and energy density across time .

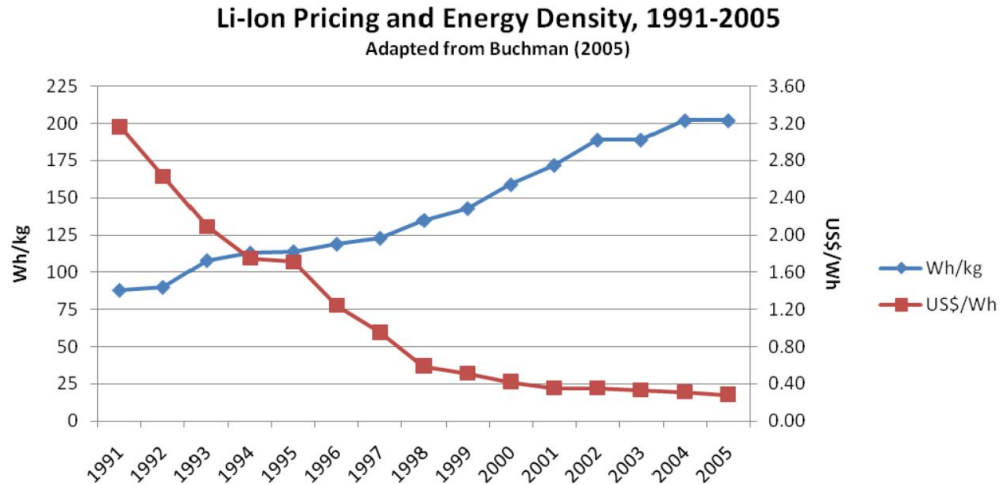


Figure 1.1: Li-Ion pricing and energy density 1991-2005. [3]

## 1.2 The centrifugal pump

A centrifugal pump is a rotating machine where the changes from mechanical energy to hydraulic is made dynamically. The way this pump deliver the energy to the fluid is by velocity changes that occur as the fluid flow through the impeller and a duct system guide the flow through the machine. Rotodynamic pump is a term used by Karassik, Messina, Cooper, and Herald; every pump that uses impeller is considered to be a rotodynamic pump, including radial flow, mixed flow and axial flow impeller, in fact the term centrifugal pump comprehends all rotodynamic pumps. Even though centrifugal pumps are three dimensional machines, it is possible to make a one dimensional analysis as the fluid moves in only one direction, therefore its possible to consider the pump a system of one degree of freedom making the calculation and study easier[4]. Among the advantages of a centrifugal pump are the easy construction and design. Very often this pumps don't require gearbox as traditional electric motors run at 3600rpm for 60hz and 2 poles. This speed can be increased or decreased with a frequency inverter, high efficient pumps use high efficient servo motors as drives, these motors use the most efficient technology to date, for example in the rotor use neodymium magnets and aluminum frames for light weight. Centrifugal pumps therefore are some of the most widely used pumps in the market. The low amount of moving parts make this pump more robust and require less maintenance. The end user to save money due to the low amount of



$$\psi = \frac{g \cdot \Delta H}{u_2^2} \quad (1.2)$$

### 1.3.2 Specific Flow - Flow Coefficient

Dimensionless number for flow rate comparison between models

$$Q_s = \frac{Q}{\Omega \cdot r_2^3} \quad (1.3)$$

### 1.3.3 Specific Speed

Geometrically similar machines larger or smaller overall dimensions, whose delivery rate is  $1m^3/s$ , at a specific energy of  $1J/kg$ .

$$\Omega_s = \frac{\Omega \cdot \sqrt{Q}}{g \cdot (\Delta H)^{\frac{3}{4}}} \quad (1.4)$$

### 1.3.4 Net Positive Suction Head (NPSH)

Local reduction of static pressure to the vapor pressure leads to the cavitation process, which can harm the blades of the machine, to describe this head reduction, the number NPSH is created. This number is measured in meters and helps to better understanding a preventing cavitation process on different machines[4]. Low NPSH also leads to pressure head loss due to the presence of water vapor in the impeller, this presence of vapor decreases density of water, therefore decreasing pressure head of the impeller.

$$\text{NPSH} = \frac{P_i n - P_v}{\rho \cdot g} = \frac{\Omega^{\frac{4}{3}} \cdot Q^{\frac{2}{3}}}{g \cdot \Omega_{ss}^{\frac{4}{3}}} \quad (1.5)$$

### 1.3.5 Cavitation Coefficient

Dimensionless number for comparison the cavitation effect between different models

$$t_2 = \frac{2 \cdot g \cdot \text{NPSH}}{(\Omega \cdot r_2)^2} \quad (1.6)$$

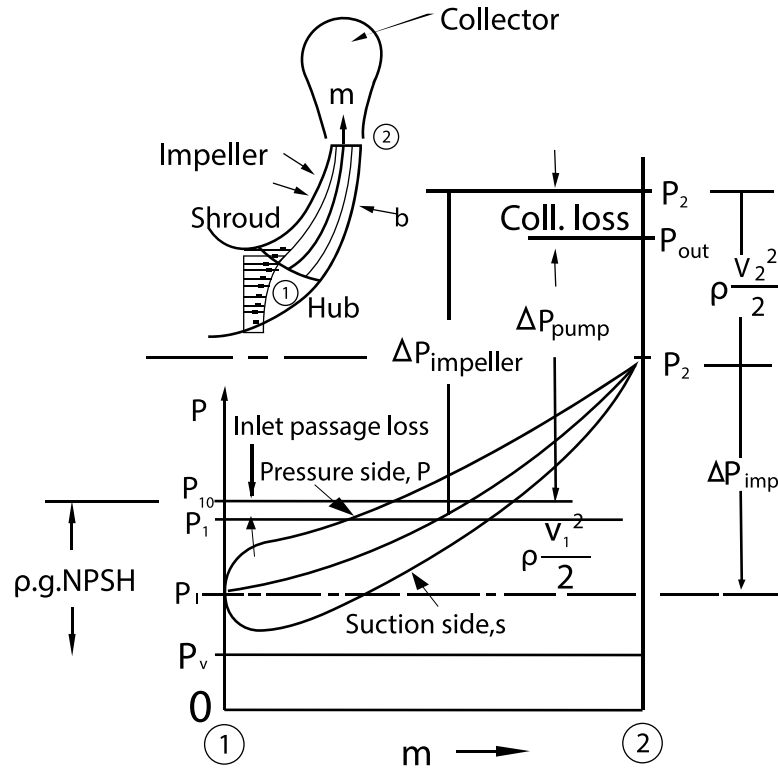


Figure 1.3: NPSH in a blade. [4]

### 1.3.6 Machine Reynolds Number

Ratio between inertial forces to viscous forces inside the machine. For high Reynolds number, the viscosity of the fluid can be neglected

$$Re = \frac{\Omega \cdot r_2^2}{\nu} \quad (1.7)$$

### 1.3.7 Classification of impellers of working machines

Figure 1.4 shows the different types of impellers, each one is defined according to the specific speed, for low specific speed positive displacement pumps are used as dynamic pumps are used in high specific speed applications. 1.5 shows the Efficiency of each impeller according to specific speed. The most efficient impeller at high specific speed are axial flow impellers. The most important parameter in a water-jet pump is thrust, therefore high flow rate impellers are used

Figure 1.6 we can see that the pump can theoretical curves and real curves. The theoretical can be found easily by fixing  $U_2$ , therefore all parameters are constant

and a line is obtained as performance curve. On the right part we can find the real curves for the pump which is first obtained by iteration from the energy continuity equation, and then fixed with performance constants to find its real shape. 1.7 shows the dimensionless performance curve of the pump

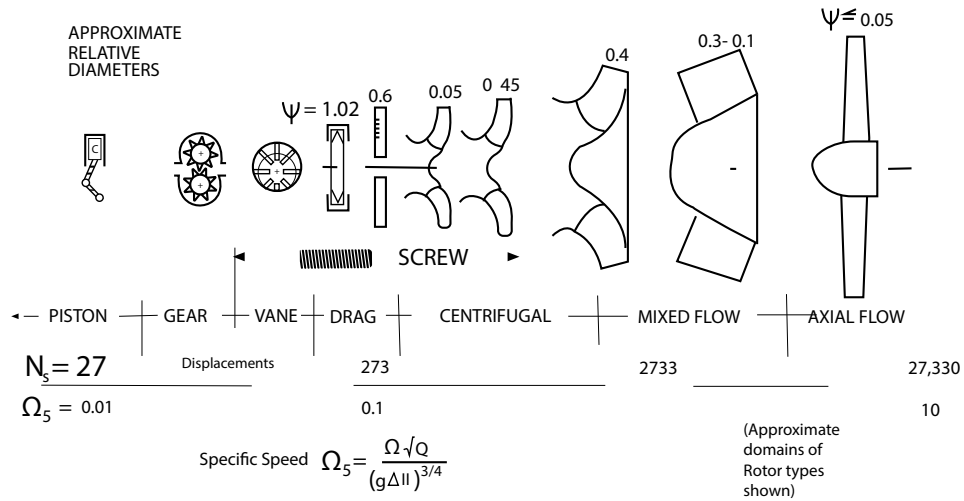


Figure 1.4: Classification of impellers working machines. [4]

### 1.3.8 Characteristics of pump

The theoretical characteristics of the pump is obtained from the continuity equation of momentum after adjustment, therefore is obtained the pressure head of the pump related to the flow rate.

$$\Delta p_{th} = \rho \left( u_2^2 - \frac{u_2 \cdot Q}{\pi \cdot d_2 \cdot b_2 \cdot \tan(\beta_2)} \right) \quad (1.8)$$

## 1.4 The Pump-Jet impeller

A pump-jet is a special pump for achievement of maximum speed of a fluid, it operates by using an axial pump to increase the water speed through an ejector and direct this water to the direction required for moving a water craft. A pump-jet therefore transforms mechanical power into hydraulic power[5].

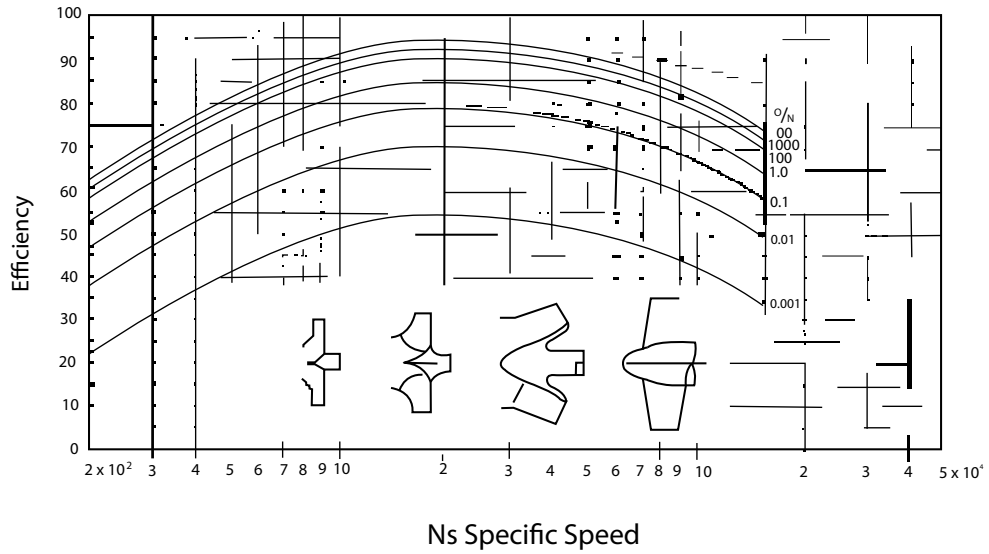


Figure 1.5: Efficiency of pumps versus specific speed. [4]

A pump-jet can be calculated as a normal axial pump. as axial pump a jet pump belongs to dynamic pumps, centrifugal, axial flow, single stage, open impeller, fixed pitch.

Dynamic pump means that energy is continuously added in order to increase fluid velocity; centrifugal means its transform centrifugal energy into velocity; axial flow indicates that inlet flow, pump axis, and outlet flow are at the same axis; single stage means it only has one impeller; open impeller means that the impeller hasn't got any housing, fixed pitch means that the shaft of rotation of the impeller doesn't change of angle respect to the axis[4].

The pump-jet system can be subdivided into two main parts, the pump and the ducting system. The pump is the drive of the system, because it transforms mechanical power into hydraulic power. The ducting system causes the exterior fluid from the inlet to the pump increasing the hydraulic power of the fluid, then to the nozzle changes the static pressure into dynamic pressure, then ducting system causes the fluid back to the environment[5].

Pump-Jet impeller is an axial impeller that has a moving head, which allows to change the direction of the boat, in Figure 1.9 is shown a prototype used for reverse engineering and analysis. This type of impeller is protected by a housing which makes it more robust. Figure 1.8 shows a simplified diagram of the Pump-Jet, notice the difference of altitude between the inlet at the pump shaft, this is due to the inlet is



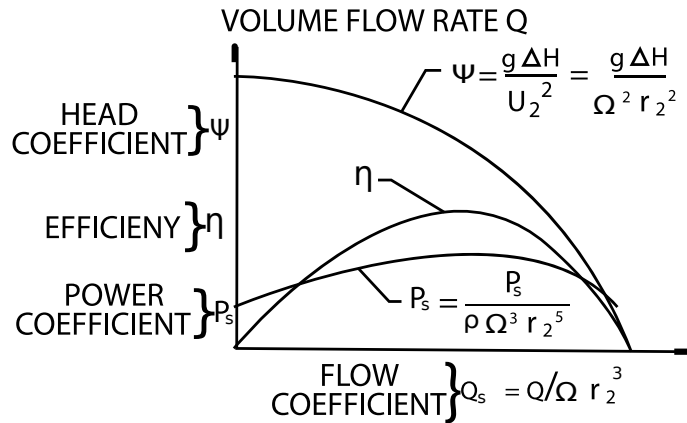


Figure 1.7: Dimensionless performance graph of a pump, relating the head coefficient and the flow coefficient. [4]

both of them must be related by using iteration in order to find the correct characteristic curve of the pump. In search for efficiency many models can be compared at the same chart allowing to choose the desired model[4].

### 1.4.2 Parameters affecting the pump-jet

Parameters that affect pumps are: inner and outlet diameter of the wheel, which will affect the pressure head of the pump, at higher diameter higher blade velocity and higher pressure head; input and output edge for the wheel affects the flow rate, moving the curve in the horizontal direction, however higher edge decreases the pressure head; angles of relative velocity at inlet and outlet affect the shape of the curve, an angle higher than 90° is called forward and produces an effect of increasing pressure head with higher angle, however the greater part of that pressure increase is found on the diffuser, therefore they require a good diffuser design, in the other hand backward blades have an angle lower than 90° (angle < 90°) which leads that the higher pressure is obtained in the impeller therefore this blades don't require good quality diffuses, the third case is called radial blade with an angle of 90° have properties between both backward and forward blades; the angle between the horizontal line, parallel to the axis and the line connecting the midpoints of flow gaps affect the type of pump that is obtained, centrifugal radial pumps have angle between 85° and 75°, axis-radial pumps have 50° angle, diagonal pumps have 45° and axial pumps have 0°.

### 1.4.3 System decomposition

The following items are a description of the system decomposition of the water jet pump diagram shown at figure 1.8, the understanding of components of the system is very important in order to calculate parameters such as energy, thrust and efficiency respect of the velocity of flow at every point of the system.

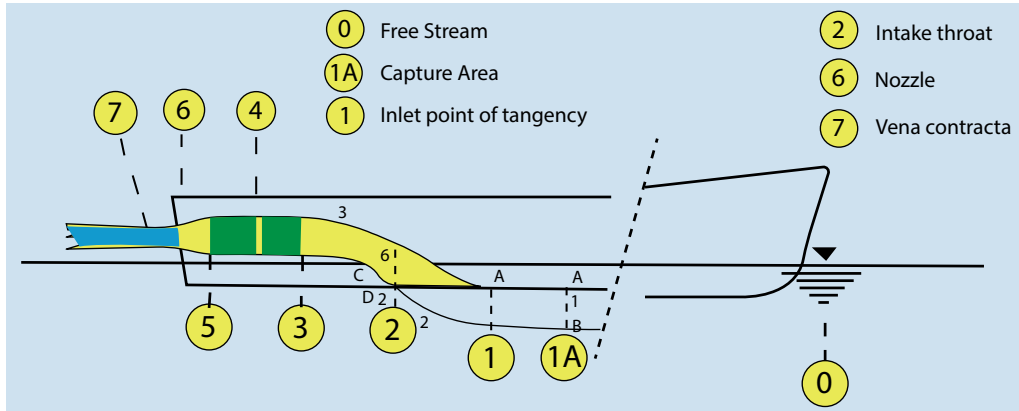


Figure 1.8: System decomposition, usage of the pump jet in a boat.[5]



Figure 1.9: A small scale prototype of the water-jet pump to be placed inside the boat as shown at Figure 1.8.

- **0 Free stream:** In this region the water flows freely, therefore the relative speed between the water and the boat is the same as the boat speed.
- **1A Capture Area :** The area of water that will be captured by the pump.
- **1 Inlet point/Stream tube inlet:** Average velocity is slightly lower than free stream due to the boundary layer reaction to the keel. Cross section area

is modelled as a rectangle 1.35 times the width of the duct pipe diameter according to rolls-Royce Standard and height is determined by the mass flow rate. through the waterjet[6]

- **2 Duct Inlet:** The water enters to the physical propulsion system, a grid or bars are installed in this point to avoid the presence of moisture that can compromise the correct operation of the waterjet.
- **3 Pump Inlet:** The pressure at this point depends on the mass flow rate of the system, the vessel speed, and the pressure loss in the duct system.
- **4 Pump center point:** After the rotor, static pressure is at its maximum, with presence of rotational flow. However Average flow speed maintains constant.
- **5 Pump outlet:** The guide blades eliminate the rotational flow, transforming it into flow axial speed.
- **6 Nozzle output:** The nozzle shrinks the diameter of the pipe transforming the static pressure into dynamic pressure.
- **7 Jet minimum diameter/Vena contracta:** The Vena contraction phenomena allows the water to be contracted outside of the nozzle reaching its minimum diameter, thus maximum flow speed is achieved.

#### 1.4.4 Water jet configuration cases

There are three cases of pump configuration: case 1 1.10 consists in an axial impeller, a guiding blade, and a nozzle, this is the standard water jet pump used in market; case 2 1.11 shows a much shorter configuration with the lack of guiding blades, hydraulic energy is lost in rotation of fluid; and case 3 1.12 which includes a hub.

#### 1.4.5 Pump jet design process

The design process flow diagram of a water jet, can be seen at 1.13. Process starts with the thrust requirements, which leads to an iterative process to find the correct pump dimensions which are limited by size, followed by the pump specifications, the energy model calculation, the blade design, steady state CFD analysis, and evaluation of results, if the results are not correct, then reevaluate the pump dimensions

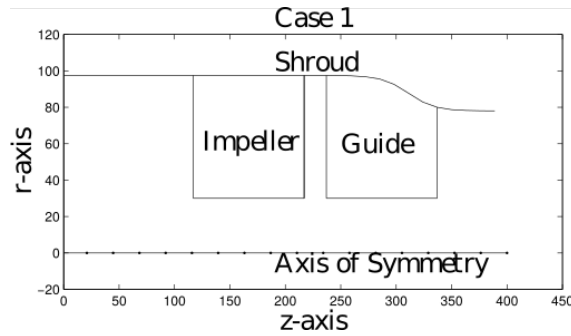


Figure 1.10: Water jet configuration case 1. [6]

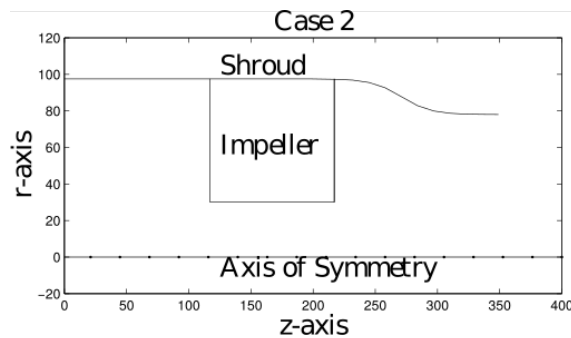


Figure 1.11: Water jet configuration case 2. [6]

and specifications. After satisfactory results, the final design is obtained altogether with the transient flow CFD analysis. Thrust requirements will be taken from the model prototype from 1.9, leading to the pump dimensions and specifications iterative process

## 1.5 Water jet equations

Water-jet has its own equations behind a regular pump, these equations are studied at ITTC(international towing tanks conference), the specialist committee on validation of Water-jet Test Procedures[5]. Equations for pump are stated for measure efficiency, thrust, and power from water jet parameters

### 1.5.1 Efficiency of a propulsor

Efficiency of a propulsor is calculated as a relation between the effective power delivered by system and the power input to system

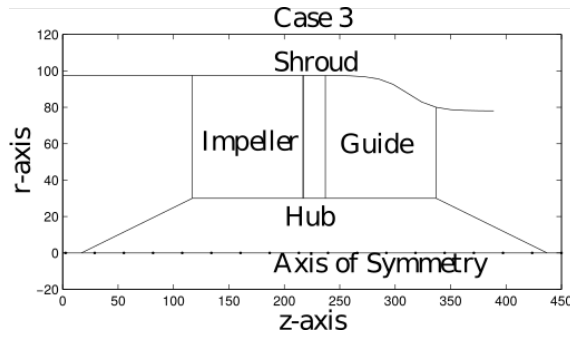


Figure 1.12: Water jet configuration case 3. [6]

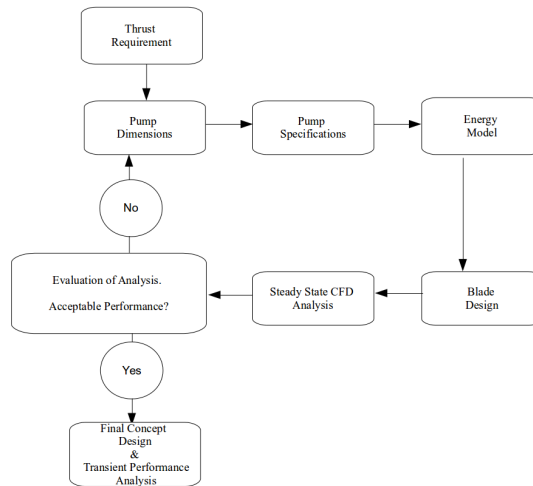


Figure 1.13: Design process of a water jet pump, based on the Rolls-Royce standard.[6]

$$n = \frac{P_{\text{outeff}}}{P_{\text{in}}} \quad (1.9)$$

### 1.5.2 Power input to system

Where the power input to the system is the sum of the effective power delivered by system and power losses

$$P_{\text{in}} = P_{\text{outeff}} + P_{\text{loss}} \quad (1.10)$$

### 1.5.3 Overall efficiency

Overall efficiency is calculated as a product between free stream efficiency and interaction efficiency

$$n_d = n_0 \cdot n_{\text{int}} \quad (1.11)$$

### 1.5.4 Nozzle velocity ratio (NVR)

Nozzle velocity ratio NVR is calculated as a relation between the velocity at point 6 of the water-jet and the free stream velocity

$$NVR = \frac{U_{\text{wj6}}}{U_{\text{wj0}}} \quad (1.12)$$

### 1.5.5 Thrust load coefficient

Thrust load coefficient (CTN) can be calculated as follows

$$C_{\text{TN}} = \frac{T_{\text{net}}}{(0.5 \cdot \rho \cdot U_{\text{wj0}}^2 \cdot A_n)} \quad (1.13)$$

### 1.5.6 Ideal jet efficiency

Ideal Jet Efficiency has many ways to be calculated, equations in 1.14 can be used independently

$$n_i = \frac{T_{\text{net}} \cdot U_{\text{wj0}}}{Q \cdot H_{\text{jse0}}} = \frac{\Delta M \cdot U_{\text{wj0}}}{E_7 - E_0} = \frac{2}{1 + NVR} = \frac{4}{3 + (1 + 2 \cdot (C_{\text{TN}}))^{\frac{1}{2}}} \quad (1.14)$$

### 1.5.7 Effective jet system

Effective Jet system power is calculated as a product of density, flow rate and the average velocity between free stream velocity and exhaust velocity of flow

$$P_{\text{JSE0}} = 0.5 \cdot \rho \cdot Q \cdot (u_{\text{exn}} - U_{\text{wj0}}) \quad (1.15)$$

### 1.5.8 Effective jet system in operation conditions

In operational conditions Effective jet system power is calculated as the difference of power at point 7 and power at point 1 of jet system

$$P_{JSE} = E_7 - E_1 \quad (1.16)$$

### 1.5.9 Model net thrust

Model net thrust is calculated as a difference between exhaust thrust and free stream thrust

$$\Delta M_x = \rho \cdot Q_j^2 \cdot A_n^{-1} \cdot \cos(\theta_N) - \rho \cdot Q_j \cdot c_{m1} \cdot U_{wj0} \quad (1.17)$$

### 1.5.10 Momentum velocity coefficient

Relation Between thrust and flow rate is calculated as a product of density, water jet flow power square, divided by area and constant called momentum velocity coefficient which is a property of every pump-jet (equation 21). This coefficient can be used as a comparison between different water-jet pumps as it relates the flow and the thrust. There are three ways to increase the thrust at a water jet pump: increase flow rate, reduce the area of the nozzle, and change the shape for increasing the momentum velocity coefficient

$$T_{jet} = \frac{\rho \cdot Q_j^2 \cdot cm6}{A_n} \quad (1.18)$$

## 1.6 Thrust Vectored Control(TVC)

Some vehicles can change the angle of thrust by using a movable nozzle, the ability of changing the angle of thrust is call thrust vectored control.[7]

## 1.7 Electrical Motor Theory

Electrical motors transform electrical energy into mechanical energy or vice versa by using the electromagnetic energy conversion property of physics[8] Electrical motors

that transform mechanical energy into electrical energy are called electrical generators, and are the base on our electrical society transforming hydraulic power, nuclear power, wind power and into electrical power which is transported using power grids to every city around the world. There are many types of electric motors which operates in different ways and require different methods to calculate its performance and control them, however all electrical motor are based on the electromagnetic force, which is one of the four forces of the universe

Three main considerations are taken into account when choosing the suitable type of motor for a certain application, these are: mechanical, electrical and thermal considerations, the main common is the standard of the National Electrical Manufacturers Association(NEMA) MG1[9], which covers frame sizing, dimensions, mounting configurations, electrical ratings, nominal speeds, and performance requirements for alternate-current(AC) and direct-current(DC) motors [8]. NEMA standards provide valuable information for most of the applications, recommending mounting configurations and defining performance ranges

### **1.7.1 Brushless Direct-Current Motors(BLDC)**

Brushless Direct-Current Motors, also known as brushless motors are a type of electrical motor which have a straight-line speed-torque curve. The rotor carry permanent neodymium magnets as the coils are stationary. Current is switched through transistors where the timing of switching is set by a circuit called “Electric Speed Controller” (ESC). There are three types of brushless motor: outer-rotor motor which has greater rotor inertia and slower acceleration, inner-rotor motor with lower rotor inertia and fast acceleration, and special-configuration motor. These motors can have one, two or three phases, where the most efficient, with reduced torque ripple effect without starting problems is the three-phase brushless motor. The number of poles of the motor depends on the requirements of speed and torque, however the greater the number of parts, the greater the amount of money the motor cost. Three-phase motor dominate the market of brushless motors, factories vary from historical to its high efficiency, two configurations are possible one called “Y” and the other called “delta” ( $\Delta$ )[8]. The power balance equation leads to the following equation

The selected motor is a brushless motor of 3650kv shown in 1.14, and the parameters are shown in table 1.1. The number 3650kv means that for every 1V it

Table 1.1: Parameters of the Electric motor selected

Description	Value
Code	DSVZ-S4005
Poles	4
KV	3650
Max current	48A
Max Voltage	16.8V/4S LiPo
Case length	50mm
Case diameter	36mm
Shaft diameter	5mm
Total length	130mm
Weight	125g

produces a rotation of 3650rpm. “Kv” is the way of measuring the electric brushless motor, therefore it’s always important to use the higher voltage to reduce the amount of electricity consumed and don’t heat up the motor.

$$K_{ta} \cdot I_a + K_{tb} \cdot I_b + K_{tc} \cdot I_c = T \quad (1.19)$$



Figure 1.14: Brushless motor selected BoatWing 3650KV.

## 1.7.2 The Electric Speed Controller[10]

For controlling the brushless motor is necessary to have an electronic speed controller(ESC), which is a special device made for controlling the speed of an electric motor. ESC’s are based on the FET(field effect transistor) to adjust the duty cycle or frequency of the create three-phase AC electrical power required to run a brushless motor. In an analog way, silicon controlled rectifiers(SCR) are used high power

Table 1.2: Parameters of the selected ESC according to the datasheet[10]

Description	Value
Model	A-SW090006
Continuous current	90A
Burst current	540A
LiPo Cells	2-6S
BEC type	Switch BEC
BEC output	5.5V/5A
Weight	102g
Dimension	57 x 49 x 18mm
Application	Boat length ; 1m

motor controllers. Which are used on high power electric industrial motors such as three-phase squirrel-cage industrial motors or three-phase industrial servo-motors which are used in industrial plants or electric vehicles. The pulse-width modulation(PWM) method is used to produce waveforms from a constant voltage source by switching on and off the transistor FET. It is the most common method implemented in practice[8]. The selected ESC is shown in 1.15 , its parameters are shown on the able 1.2 according to its datasheet[10].



Figure 1.15: Flycolor ESC A-SW090006 for 90A.

## 2 CFD methods

The Computational Fluid Dynamics(CFD) is a method for making analysis of the fluids, in [11] they called “The Third approach” , before the year 1960 only theoretical equations were used for designing machines such as airplanes or pumps. After those years with the advance of electronics, computers, develop software and research the CFD started to become more important on engineering.

The CFD comprehends different ways for solving the Navier-Stokes equations, each computational method has its advantages however the most important parameters to consider in every CFD calculations are quality of results and computational cost. Steady flow analysis has the lowest computational cost and helps to have fast results when designing a pump helping rapid model iteration. After the iteration process, its possible to change the analysis to transient flow in order to have more accurate results[6].

### 2.1 Theory

#### 2.1.1 Pre-processing

##### ANALYSIS

**Steady state** This is the most cost-effective analysis due to its fast and accurate results, serves for the basic analysis of the pump when iteration process of model parameters is in basic state. This analysis is independent of time, therefore considering flow as steady. The rotation of the impeller is modelled as a rotation of the grid around the impeller blade. A drawback of this analysis is that the guide vane must be considered at constant position respect impeller blade as the time is constant[6].

**Transient** This analysis solves the Navier-Stokes equation for time dependent unsteady flow with the drawback of high computational cost. The result shows the unsteady flow analysis across time. As the impeller rotates it shifts its position in relation to the guiding blades. This model analysis is therefore more accurate than steady state[6].

## PREDICTION OF WALL DURING TURBULENCE

For dealing with turbulent flow, two approaches are made, first one is integration of turbulence wall, and the other way is called wall functions, the usage of these two methods depend on the value of a parameter called Y-plus.[12]

Y-plus is the size of the first cell at a wall, resolution of boundary layer must be fine enough to ensure y-plus size is good for the turbulent model. For research standard y-plus value must be less or equal than 1, however an industry standard requires only a y-plus of 30-60, making it the right choice due to its low cost and high benefit ratio[6].

**Integrate turbulence of the wall** The turbulent model is modified all mesh down until the viscous layer, this method requires a lot of computational resources due to the amount of mesh cells. The first cell center must be placed on the viscous layer, preferably  $Y^+ = 1$ . A low resolution model such as k-omega can be used.[12]

**Wall functions** Wall functions are empirical functions that can solve the area between wall and turbulence fully developed region, this helps to reduce the amount of mesh cells used thus allowing faster and more accurate results. First cell grid requires to be  $30 < Y^+ < 300$ . High resolution models can be used such as k-epsilon. [12]

## FLOW MODELS

**SST k-omega Turbulent** The turbulent flow in steady and transient state analysis is modeled using SST(Shear-Stress Transport) k-omega turbulent flow model. This model was proposed by Menter in 1992[13]. The model is a combination between the model k-epsilon which works well with free stream flow, with the drawback of the requirement of a damping function for analysis near the wall; and the Wilcox k-omega model which works well by analyzing flow near the wall with drawback of

free stream flow stability. Combining these two models takes the best of each for free stream flow and near the wall stability, for more information check the [6] and [14].

For flow analysis, it is important to calculate the shear viscosity property, which consist on the sum of collision therm, kinetic therm and friction therm.

$$\mu_l = \mu_{l,\text{coll}} + \mu_{l,\text{kin}} + \mu_{l,\text{fric}} \quad (2.1)$$

Each of these therms can be modeled according to many equations according to local particle volume fraction, density of particle, particle diameter, radial distribution function, particle restitution coefficient and granular temperature. These equations are available in the software ANSYS FLUENT by default.[15]

**Mixture** The mixture flow model performs a multi-phase analysis of fluid. From the three states of matter: solid, liquid, and gas; this model is able to calculate more than only liquid as fluid. In case of pumps we require to calculate the liquid-phase, as well as the presence of gas-phase in the pump.

This helps to analyse the presence of cavitation in the pump as in cavitation process there is presence of vaporized water which decreases the pressure head of the pump and damage the impeller. Turbulent flow model is added to the analysis where the two phases defined as liquid and vapor are defined together with a transfer function. This function defines cavitation to a given vapor pressure. According to ANDERSEN [6], this model is difficult to use for large amount of vapor, therefore a first order scheme is used in order to calculate the volume fraction and momentum equation thus increasing stability with the drawback of decreasing model accuracy. This model is a good method to measure and prediction of cavitation on the pump. Cavitation analysis is usually adjusted in order to match experimental results[6].

## SCHEMES

Upwind schemes are discretization methods for solving Hyperbolic partial differential equations. They use finite difference method for solving the propagation of information through a flow field.

$$u_i^{n+1} = u_i^n - \Delta t(a^+ u_x^- + a^- u_x^+) \quad (2.2)$$

**First order upwind** The most basic upwind scheme.

$$u_x^+ = \frac{(u_{i+1}^{n+1} + u_i^n)}{\Delta x} \quad (2.3)$$

**Second order upwind** The second order upwind scheme is used in steady and transient flow analysis. As the flow in a water jet pump is mostly axial, the second order upwind scheme is a good choice due to its stability and second order accuracy of results. Implicit scheme is used in discrete time analysis over transient flow analysis. First order upwind is used for the momentum and volume calculation at cavitation analysis, it's important to say that first order is faster and requires less computational resources than second order[6].

$$u_x^+ = \frac{u_{i+2}^n + 4u_{i+1}^n - 3u_i^n}{2\Delta x} \quad (2.4)$$

**Third order upwind** The most accurate upwind scheme, requires a lot of computational resources.

$$u_x^+ = \frac{-u_{i+2}^n + 6u_{i+1}^n - 3u_i^n - 2u_{i-1}^n}{6\Delta x} \quad (2.5)$$

## Meshing

Meshing process is a discretization method of the domain for the FVM(Finite Volume Method). CFD meshing it consists in the creation of cells considering computational resources to be deployed, the capacity of the computer both according to hardware and software as well as the resolution increase near walls. An example of mesh can be seen at 2.1.

### 2.1.2 Processing

Consists on solution of the geometry with the given parameters on last step.

## SOLVER ALGORITHMS

**SIMPLE** The SIMPLE algorithm is an acronym for Semi-Implicit Method for Pressure Linked Equations. It is an iterative, stable, cost efficient, algorithm to solve pressure and velocity. SIMPLE introduces the “guess & correct solver approach” increasing stability. This algorithm solves individual cells one by one allowing low ram memory computers the possibility to run this solver. A modified version of the algorithm allows transient flow analysis[6].

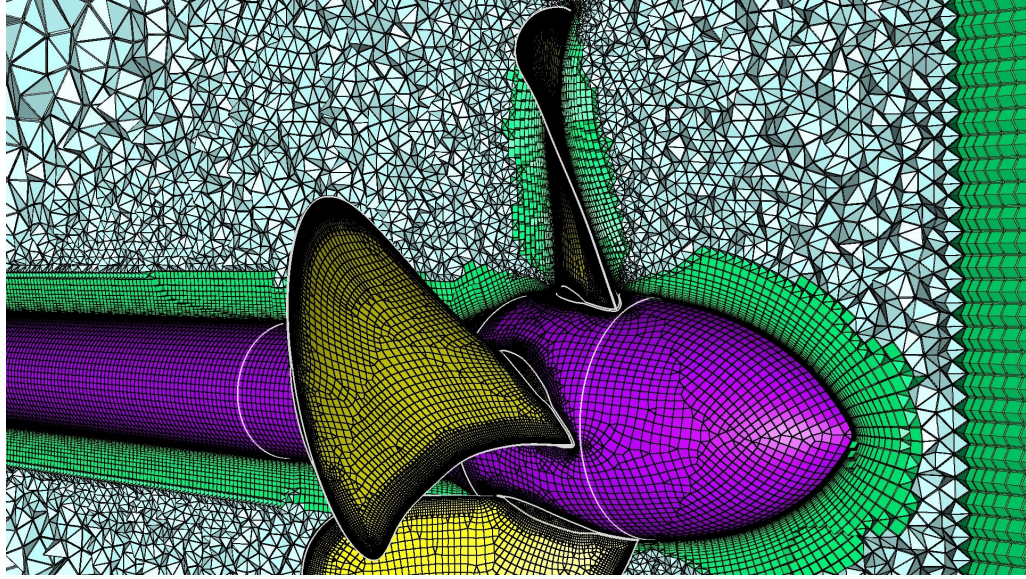


Figure 2.1: A mesh example of a propeller. [16]

**PISO** The PISO (Pressure Implicit with Splitting of Operators) is a method for solving the Navier-Stokes equations. In this algorithm no under-relaxation is applied, and the momentum corrector step is applied more than once[17].

### 2.1.3 Post-processing

During post processing, results will be observed and presented in to be reviewed. The presentation of results depend on the software used.

## 2.2 Specification of the problems

### 2.2.1 Flow

For this project, high thrust is required, therefore a turbulent flow is expected to be achieved.

### 2.2.2 System

Due to the presence of turbulence, theoretical model might not be very accurate. The system has a cavity that has irregular shape, which increases cell skewness.

## **2.3 Solution**

### **2.3.1 Flow**

This will require special effort when meshing near the walls using the command inflation as well as sweep body meshing methods. Turbulent model will be set for viscosity calculation.

### **2.3.2 System**

Multiple design points will be set alongside with many models in order to find the most suitable one. System will be separated in blades, nozzle and intake for setting the most accurate meshing methods where possible.

### **2.3.3 Computational mesh**

Computational mesh is generated by the ANSYS tool Workbench, mesh is refined at the walls to ensure accuracy at boundary layers, blades are considered walls but modelled as with smaller cells due to blades complex geometry and the requirement of low y-plus values. Remaining domain is generated as unstructured mesh. A grid study is performed to ensure sufficient grid independence[6].

### **2.3.4 Convergence**

For water jet pump design, calculation convergence can be defined as a minimum reduction of a factor for the residuals and a maximum fluctuation of 1% of the torque over 200 iterations[6]. However in this project number of iterations will be reduced to 100 due to the capacity of the computer, number of design points, number of models, time, model and high resolution of mesh.

### **2.3.5 Post-processing**

CFD post is a tool to visualize the CFD calculations performed by the software ANSYS[6].

## 3 Software

### 3.1 ANSYS

It's a simulation software for CFD(Computational Fluid Dynamics) prototyping, among it's capabilities are CAE(computer aided engineering), and CFD[18]. The main benefit of these software for engineering is the intuitive user interface that helps to separate the settings, for example in this project the following modules have been used:

- Model(Imported from Creo4)
- Mesh
- Fluent
- CFD post

### 3.2 MATLAB

Matlab is a programming platform designed for engineers and scientists, it allows to analyze data, develop new algorithms as well as to create models and applications[19]. The software has many built-in mathematical functions as well as some tool-kits that help to arrive to the solutions really quickly. With the coding its possible to read data in files, store them in vectors and process them. The iteration ability helps to converge models really quickly and the plotting allow to store the results in images at any quality and format required. The programming language is easy to use and to learn, few hours are required to master a top-level language like MATLAB, with the ability to fully control the size of the variables, and the type of them. The toolkits help the user to find the solutions to faster with the drawback of not knowing the exact process of the solution.

### 3.3 GNU Octave

GNU Octave is a free Open source software partially compatible with MATLAB[20], it contains the same programming functions as MATLAB with small changes due to copyright, the Octave interpreter can be run in GUI mode, as a console or invoked by another program. Free Open Source software means the code of the software can be reviewed by any person in the world, and it's modified by a community of volunteers around the world which keep the software always in maintenance adding new features and creating new versions of the software. The flexibility of the software makes it smaller than it's counterpart, making it faster for small and medium sized machines. Its requirements are much lower than other private software which makes it easier to be installed and used[20].

## 4 Experimental methods

### 4.1 Thrust measurement with load cell

A load cell is a type of transducer, transforming kinetic energy into electrical energy. The output electrical signal can be further measured thus obtaining values such as force tension, compression, pressure or torque. There are three types of load cell: hydraulic, pneumatic, and strain gauge. The high precision, low cost makes the gauge load cell the most common load cell available in the market. The strain gauge load cell is made of a solid metal body called “spring element” where the strain gauges are placed, body material can be steel or aluminum in order to minimize the deformation[21]. Once the strain gauges changes its shape its electrical resistance changes with the deformation, special electrical circuits such as the micro component HX711 are made for processing the electrical resistance change in the strain gauge allowing the data to be processed later using a computer[22].

Figure 4.1 shows the block diagram of the module HX711[22] it can be observed that the module can be powered by a wide voltage range of 2.7V - 5.5V, the digital outputs lead to a high quality result of measurement from the load cell. The internal 24-bit ADC means that the signal amplified by the gain is divided in 16777216 parts, this process ensures the high quality of the measurement. Figure 4.2 shows the 5Kg load cell that will be used for measurement, the red cable is the power cable, the black cable is the ground cable, and the green and white cables are the sidelines outputs of the Wheatstone bridge circuit used on the strain gauges attached to the load cell for measurement.

### 4.2 Power measurement

Electrical power can be measured by measuring the current flow and multiplying by the voltage(Joule law). As a brush-less motor can use a great amount of electrical

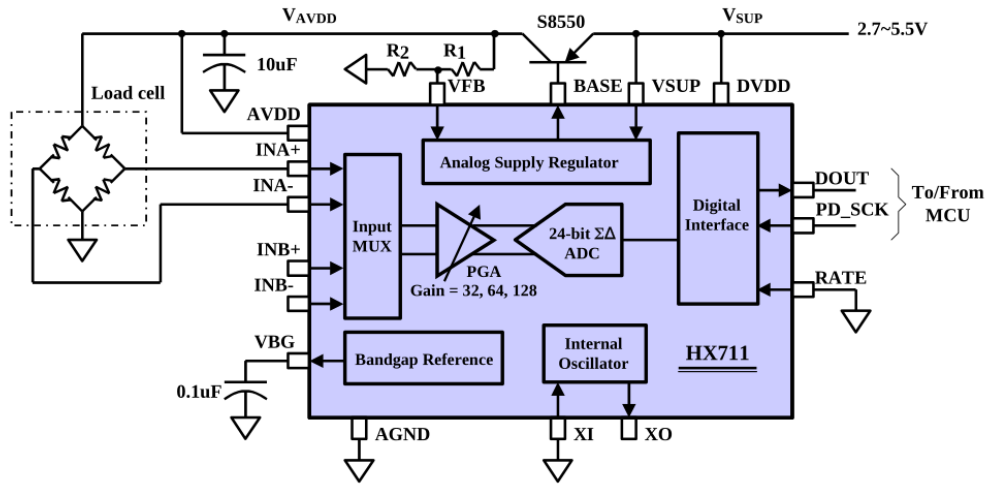


Figure 4.1: HX711 sensor.[22]



Figure 4.2: Load cell picture.

current, a special type of sensor is required, chosen sensor is the ACS758[23] which has the ability to measure electrical current up to 200A with a precision of 0.1A at 25° C with a test current of 50A for the version X050U, giving the sensor a precision of 0.2% of error towards the measurement. The sensor creates an output of analog voltage which can be measured by any device and further processed by a computer. Figure 4.4 shows the diagram of the module with its respective pin-out, as it can be observed, the module can be powered at 3.3V as 5V. Pin 4 and 5 are the terminals to current measurement, some models of this module allow the current to pass in both directions. The minimalist design of the module, and the small amount of components required for function make this module affordable.

It is possible to use other types of electrical measurement, such as using a manual multi-meter, or non invasive sensors. However this other configurations will lead to error when measurement as well as price increase. It's more optimum to measure all

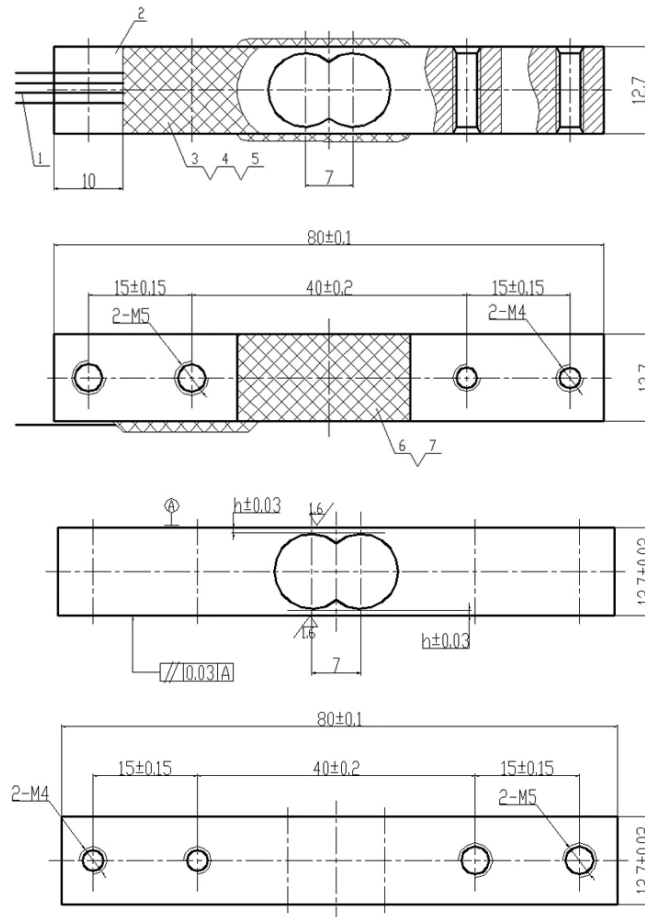


Figure 4.3: Load cell drawing.

the variables with the same computer at the same time to get the greater amount of empirical data possible to have a good mathematical model of the pump prototype. A drawback of this sensor is the analog characteristic of its output, which requires calibration and can lead to an error, where more complex sensors by having a digital output can be more accurate. The analog conversion also leads to the loss of computational resources on the MCU.

### 4.3 Microcontroller Unit (MCU)

According to [24], the first company to design a Micro-controller was Texas Instruments(TI), combining a microprocessor and the other IC's like RAM's and ROM's in the same chip. Gary Boone and Michael Cochram succeeded creating the first Micro-controller in 1971. The TMS 1000 low price helped it to become the most

Table 4.1: Load cell parameters

Description	Value
Range	1-10kg
Output sensitivity	1.0+-0.1mV/V
Zero output	+/-0.1mV/V
Nonlinear	0.05% F.S
Lag	0.05 % F.S
Repeatability	0.05% F.S
Creep	0.05% F.S/3min
Output impedance	1000+-5% ohms
Zero temperature drift	0.05% F.S/10C
Temperature sensitivity drift	0.05% F.S/10C

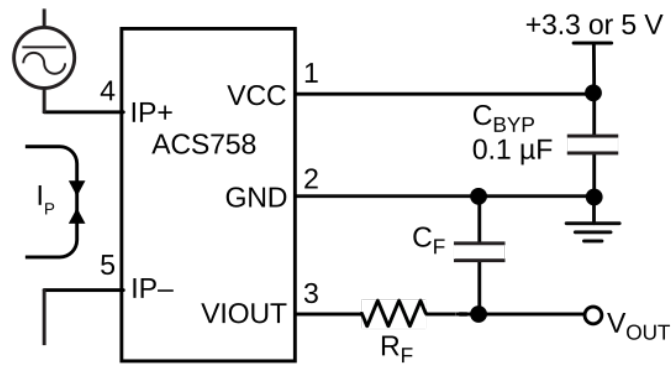


Figure 4.4: Electric current sensor ACS758.[23]

popular Micro-controller at the time, making it a success on the consumer electronics such as calculators, toys, games, alarms, photocopiers machines and more. The TMS 1000 made electronics available to everyone at the time. The ESP32 is a 2.5GHz WiFi and Bluetooth chip with 40nm technology, it is designed for low power consumption applications, with high versatility and high number of applications. It uses a 32bit LX6 Xtensa microprocessor with 520kB of RAM memory, as well as 448kB of ROM, with a internal oscillator of 8MHz. Main features of this Micro-controller are it's 34 programmable General purpose input output(GPIO) pin-out, its ports for communication SPI,  $I^2C$  and UART[25]. These capabilities will help to process the information that comes from the sensors such as 4.4 and 4.1 attached

to the prototype 1.9. Thanks to the Bluetooth and WiFi capabilities, the system will be programmed over the air(OTA), which allows to upgrade or change firmware without physical access within minutes, without any interface [26].

## 5 Results

### 5.1 First Approach

First approach consists in perform regular calculations of pump speed, flow rate, thrust, cavitation and performance. For this section the software Octave was used in order to perform the calculation iterative. The function can be found in the attachment [A1](#) of this file. Design process will be as follows:

1. Perform calculation of the electric motor speed according to duty cycle and battery voltage.
2. Perform a first simulation with a model considering a second stage in order to evaluate change of performance and parameters
3. In order to find new values of a model, its important to evaluate the changes of every parameter according to blade diameter, nozzle diameter and blade angle.

#### 5.1.1 Electric motor

Figure [5.1](#) shows the theoretical linear relation between speed of the electric motor in revolutions per minute and it's duty cycle using a Li-Po battery of 14.8V.

$$Speed_{motor} = Duty \cdot V_{Battery} \cdot K_V \quad (5.1)$$

where  $Speed_{motor}$  is the motor speed in *rpm*,  $Duty$  is the duty cycle set to the controller,  $V_{Battery}$  is the battery voltage (14.8V), and  $K_V$  is the brush-less motor speed constant.

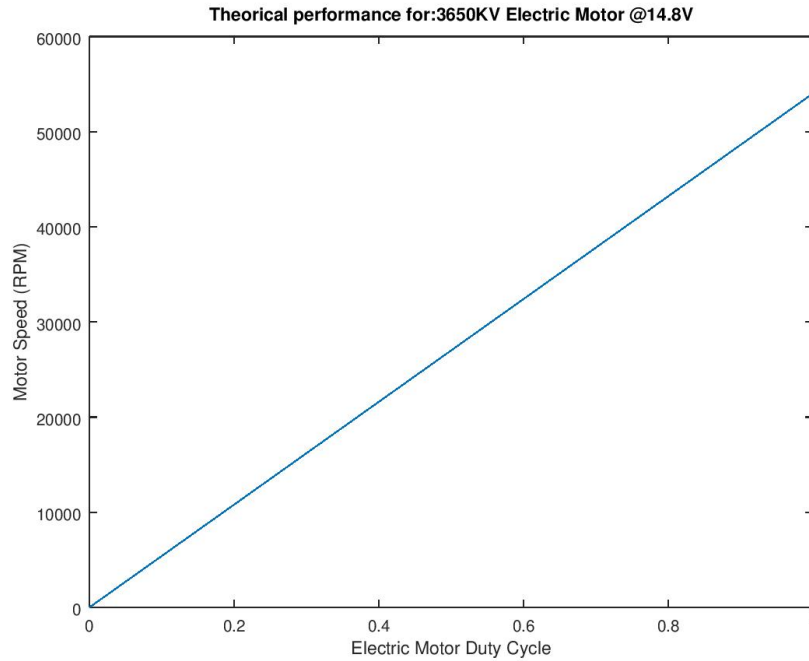


Figure 5.1: Electric Motor Calculation.

### 5.1.2 Model dimension measurement

In order to perform calculations of the model 1.9, inner cavities are measured and shown in table 5.1. Figure 5.2 shows the two stage model v0.

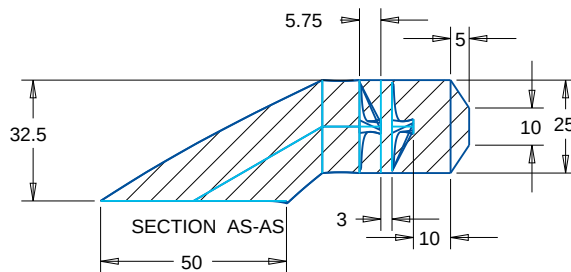


Figure 5.2: Water-Jet model in CAD

### 5.1.3 Comparison between model and proposed design

Model shown in Figure 1.9 has rotating blades and guiding blades for elimination of rotating component in water flow. Proposed design consists in a second stage counter-rotating blades to decrease the size while maintaining motor speed and thrust.

Figure 5.3 shows the relation between pump dimensionless numbers according to motor speed. Head coefficient, Specific Speed and Cavitation coefficient are constant values due to the constant motor torque of an electric machine, and the performance of a axial water pump. Head coefficient, NPSH and Cavitation coefficient are remain constant in proposed design, while Specific speed increases.

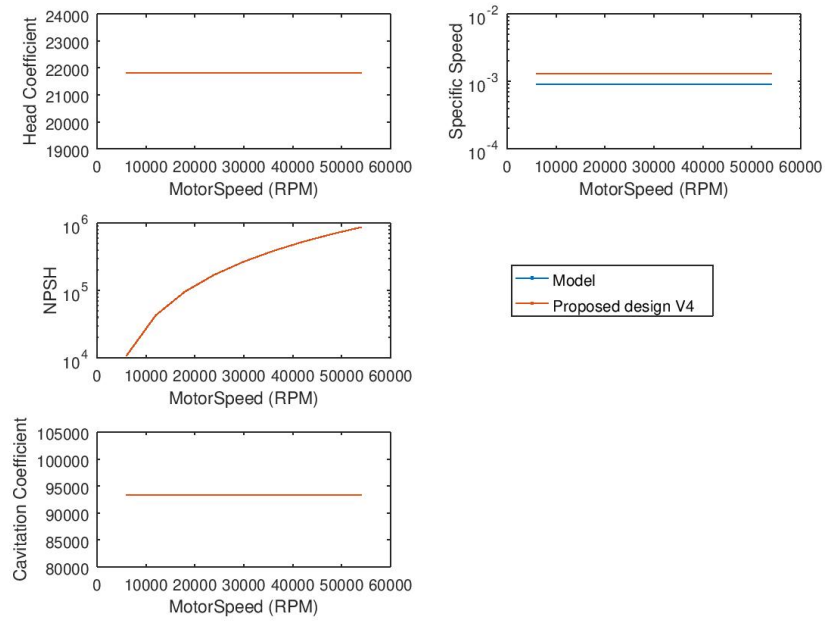


Figure 5.3: Water-Jet Calculation, pump approach and cavitation analysis.

Figure 5.4 shows the comparison between old-model and model version-4, showing dynamic pressure, thrust, thrust load coefficient(CTN), theoretical jet efficiency, nozzle velocity ratio(NVR) and momentum velocity coefficient(cm6); as expected the proposed design increases all values except the ideal jet efficiency.

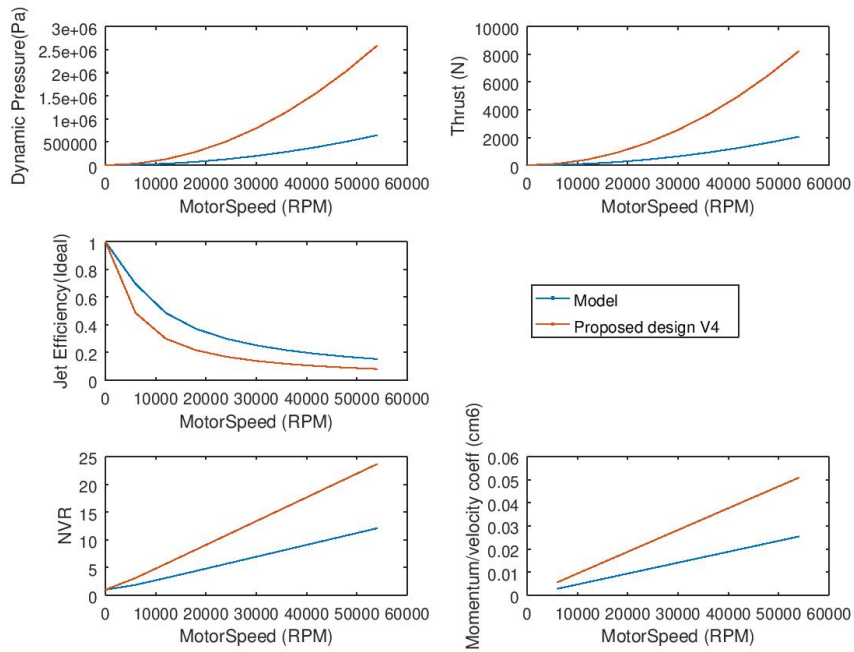


Figure 5.4: Water-Jet Pump Calculations and performance comparison.

## Optimization

As seen in Figure 5.4, the proposed design has more thrust and less theoretical efficiency than model. This is due to shape is not optimized, diameter of blades, nozzle diameter and blade step must be changed in order to achieve the same thrust. According to the Water-Jet equations, blade diameter and nozzle diameter can be reduced while keeping the thrust, thus reducing the size of the Water-Jet.

By recalculating the performance in a pump approach and water-jet approach we can measure new values for comparison between old-model and model v0. Figure 5.5 shows head coefficient and cavitation coefficient have increased in proposed model v0, while specific speed decreased. NPSH remains constant.

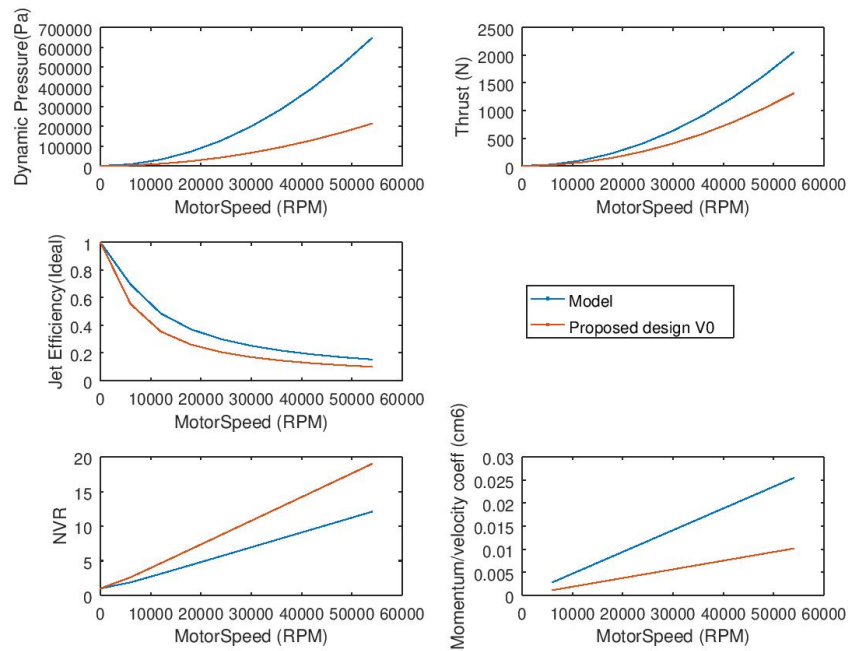


Figure 5.5: Water-Jet version 0 pump calculations and performance comparison.

However Figure 5.6 shows dynamic pressure is decreased, while jet efficiency curve is slightly lower as well as thrust while CTN and NVR values are greater. These values must be compared with CFD simulations in order to get real pump efficiency values and therefore improve the values.

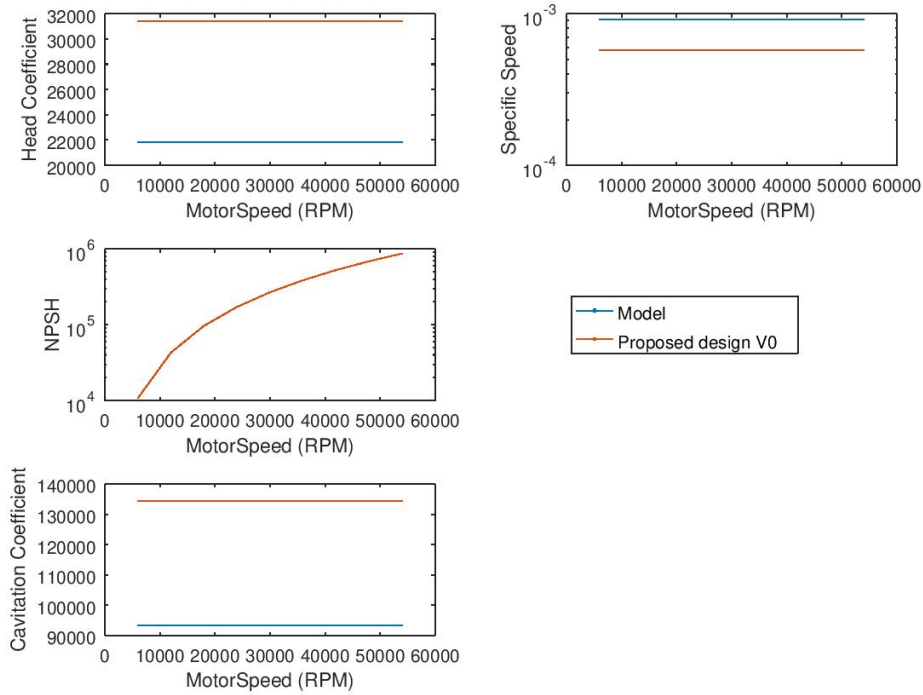


Figure 5.6: Water-Jet version 0 calculation, pump approach and cavitation analysis.

### Nozzle and Blade sizing

Figure 5.7 shows the relation between blade step and diameter for different design nozzle sizing, as seen value of blade step can be found from diameter, therefore blade angle can be found from the relation of these two values. This allow the simplification of mathematical calculation for constant thrust. For calculation a vehicle speed of 7m/s is assumed. Blade step has been calculated using the following equation which is a derivation of thrust conservation:

$$Step_{new} = \frac{D_{old}^2 \cdot Step_{old} \cdot Nozzle_{new}}{2 \cdot D_{new}^2 \cdot Nozzle_{old}} \quad (5.2)$$

where  $Step$  is the step of the designed pump,  $D$  is the pump diameter, and  $Nozzle$  is the nozzle diameter.

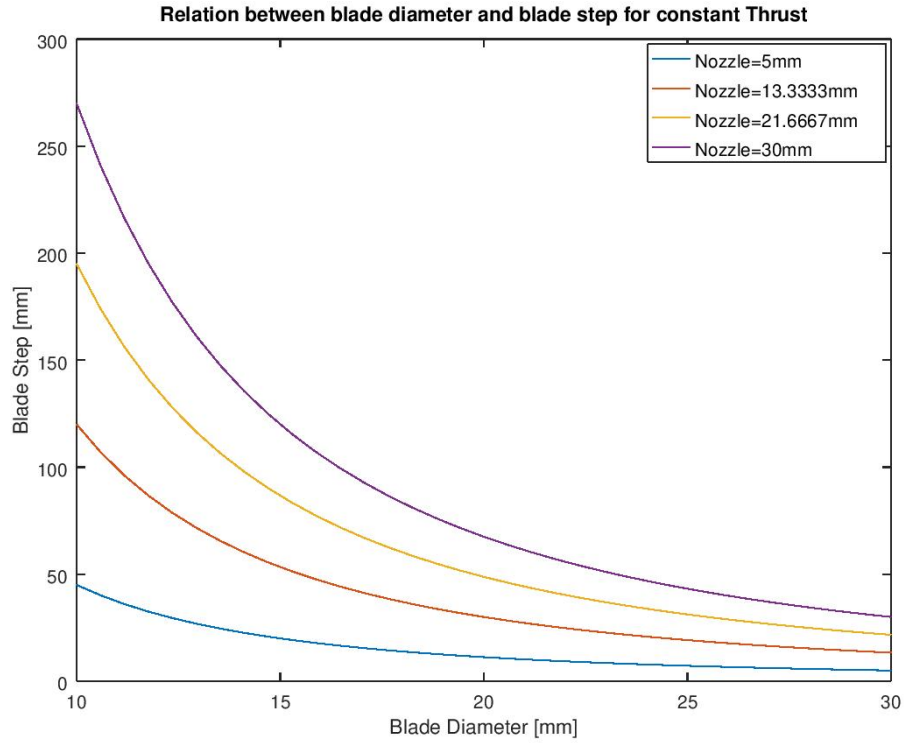


Figure 5.7: Water Jet calculation blade step-diameter relation.

Figure 5.8 shows the size effect in different pump values, dynamic pressure increases by decreasing blade size due to conservation of flow rate. CTN value increases for low nozzle size. Jet efficiency increases according to nozzle. Bigger NVR value increases inversely to nozzle, while cm6 value maintains constant. Thrust of the jet remains constant with nozzle diameter.

Figure 5.9 shows head coefficient increases by lowering blade diameter, as well as cavitation coefficient while NPSH and specific speed values remain constant. From these calculations we can redefine nozzle diameter to 10mm because even though jet efficiency is quite low, thrust value remains constant. More accurate values of thrust will be calculated using CFD.

Different sizing of models can be found in Table 5.1, these values shown that approximately the blade diameter and step are the same size, therefore for maintaining the blade angle the new model will maintain the size relationship also.

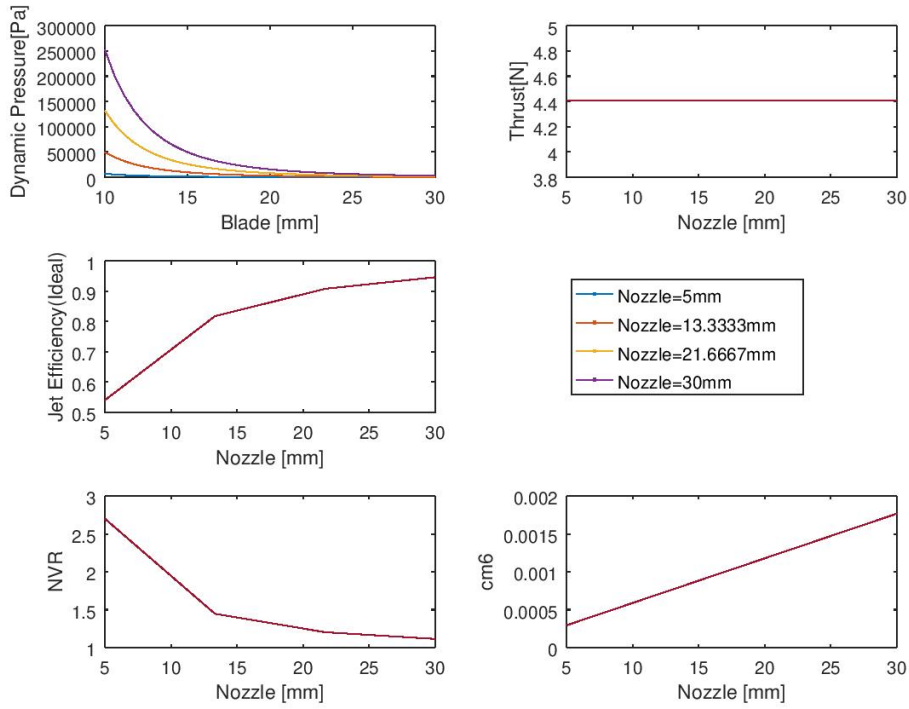


Figure 5.8: Water jet calculation performance comparison by size.

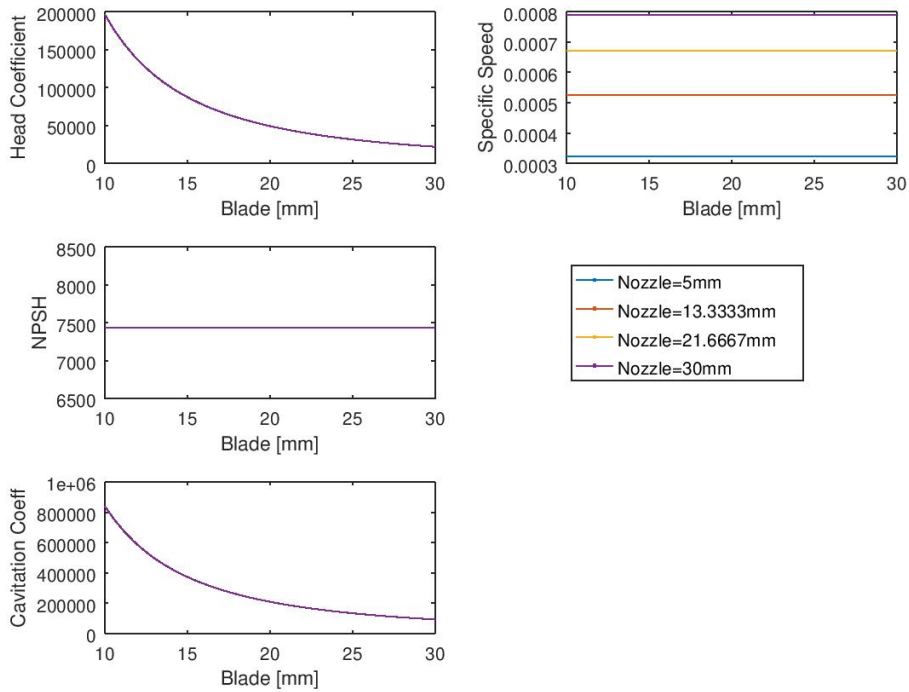


Figure 5.9: Water-Jet pump calculations and performance comparison by size.

Table 5.1: Parameters of different Water-Jet pump models

Description	Blade D [mm]	Nozzle D [mm]	Step/4 [mm]	Stages
Old Model	30	20	10	1
V0	25	10	5.75	2
V3	30	10	10	2
V4	30	20	10	2
V6	25	20	5.75	2

## 5.2 CFD Analysis

CFD analysis is made using k-epsilon turbulence model, over 1000 iterations considering effect of gravity. Transient analysis is considered

- Working Fluid: Water(properties default from fluent material database)
- Wall material: Aluminum(properties default from fluent material database)
- Gravity effect: yes

### 5.2.1 System assumptions

Gravitational acceleration is considered as 9.81m/s, as well as dynamic pressure produce by boat speed is modelled as an increase static pressure at inlet of pump.

### 5.2.2 CAD Modelling and designs

CAD models were designed using CREO4 software, parameters are shown in table 5.1. Figure 5.2 shows the two stage model v0.

### 5.2.3 Meshing

For meshing the software Ansys Meshing is used with the following options:

- CFD method
- Target skewness 0.8
- Number of cells greater than 100 000

Table 5.2: Design Parameters

INPUT	OUTPUT
Pressure inlet[Pa]	Mass flow rate[kg/s]
Blade Speed[rpm]	Fluid outlet velocity $U_{wj6}$ [m/s]

- Sweep meshing method where possible.
- Wall region inflation: program controlled

## 5.2.4 Boundary Conditions

By default Ansys Fluent sets all exterior boundaries as wall, which in this case is defined as an Aluminum wall. Internal fluid is set to be water, however Blades have a rotation axis and angular speed.

In order to set different inlet pressures and different blade speeds, Design point parameters are set. Design points are parameters set at Ansys workbench in order to change quickly boundary condition parameters externally of the system. This method allows to perform multiple simulation sequentially. Table 5.2.4 show the design parameters for inlet and outlet for every design point.

In the figure 5.10 it is possible to see the water tank and the water jet. Pressure inlet is located at the bottom face of the tank, while pressure outlet at 0Pa(atmospheric pressure) is located at the end of the nozzle.

## 5.2.5 Design points

The speed of the watercraft is set to be [0 - 7]m/s as well as the motor speed is set to [0 - 60 000]rpm; in the case of two staged models, motor speed is the same for both stages but second one has opposite direction. Inlet pressure is found with following equation:

$$P_{inlet} = P_{static} + 0.5 \cdot \rho \cdot V^2 \quad (5.3)$$

where  $P_{inlet}$  is inlet pressure,  $P_{static}$  is static pressure at 0.1m deep in water,  $\rho$  is density and  $V$  is the velocity of fluid. Therefore the inlet pressure is set to be [2972, 13440, 25404]Pa. The motor speed is set to [5000, 10000, 30000, 60000]rpm. Therefore 12 design points are obtained.

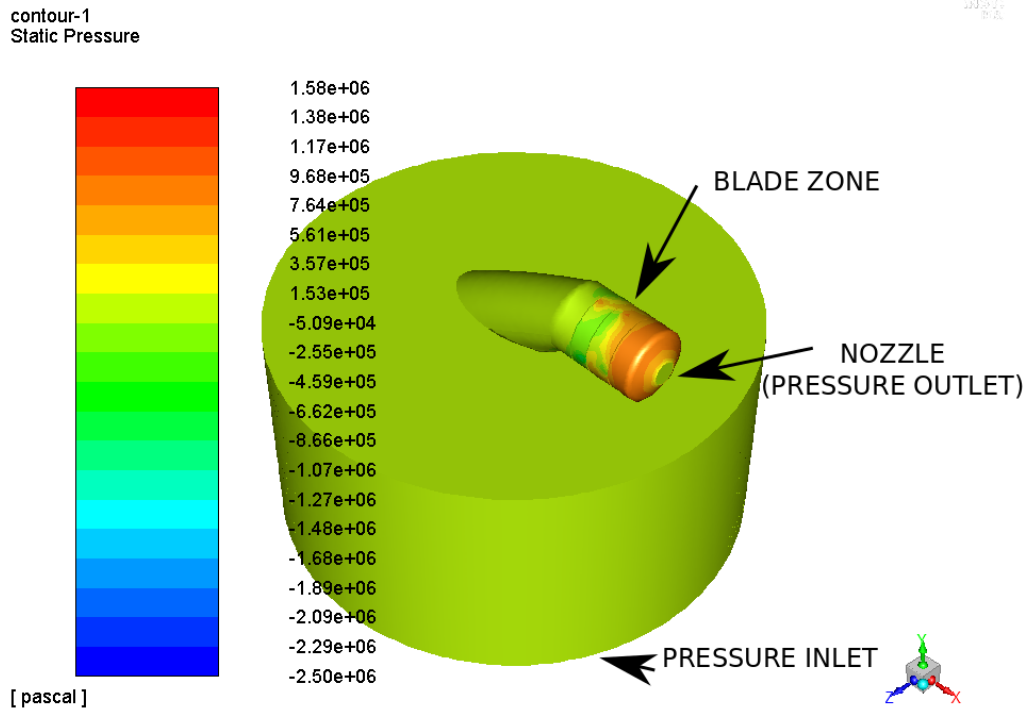


Figure 5.10: CFD experiment with tank.

### 5.3 Experimental Analysis

In order to obtain experimental data, it's required to mount the water-jet pump into a frame as seen in 5.11, the blue parts are the 3D printed adapters between the model, the load cell in red color, and an aluminum profile 2020 frame. This system must be places in a water tank, circuits must be carefully isolated in order to prevent causing short circuits.

The experiment consists in perform proper wiring of all sensors described in previous chapter, the load cell will measure thrust[N], the current meter ACS758 will help to measure power by multiplying its current value to voltage of battery. All this process will be controlled with a module ESP32 capable of wireless programming through WiFi(Over-The-Air programming). The Full experiment lasts 30 seconds thus collecting data using a low pass filter: average filter. Data will be stored every 10 milliseconds during the experiment. Duty cycle of electric motor will change from 0 to 1 during these 30 seconds thus obtaining 3000 points for the values of: Electric current[A], Duty cycle[-] and Thrust[N].

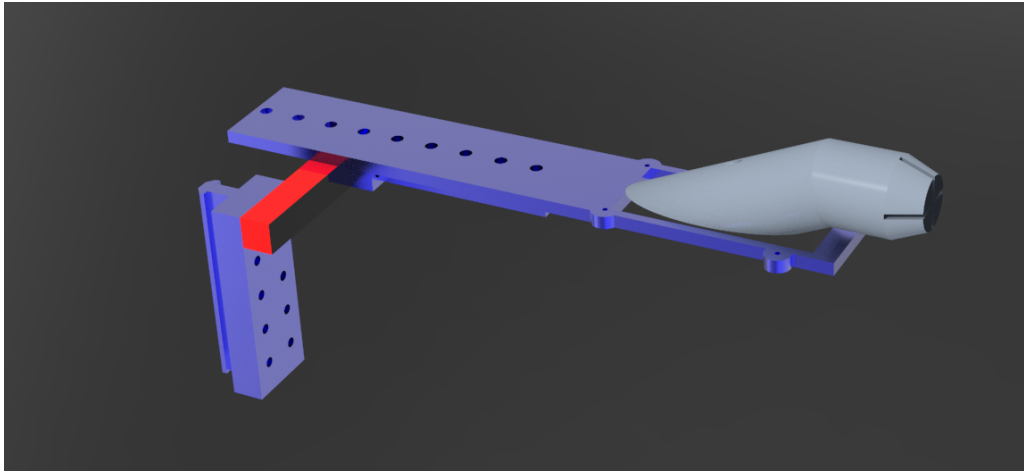


Figure 5.11: Experiment sketch of pump model mounted in frame. a) In Blue: 3D printed adapter parts. b) In Red: Load cell. c) In Gray: Water jet pump model.

Figure 5.12 shows the wiring of the selected components. Connections are shown in different colours showing power cables(Red), data wiring(Black), wireless communication(Blue) and Mechanical coupling(Green).

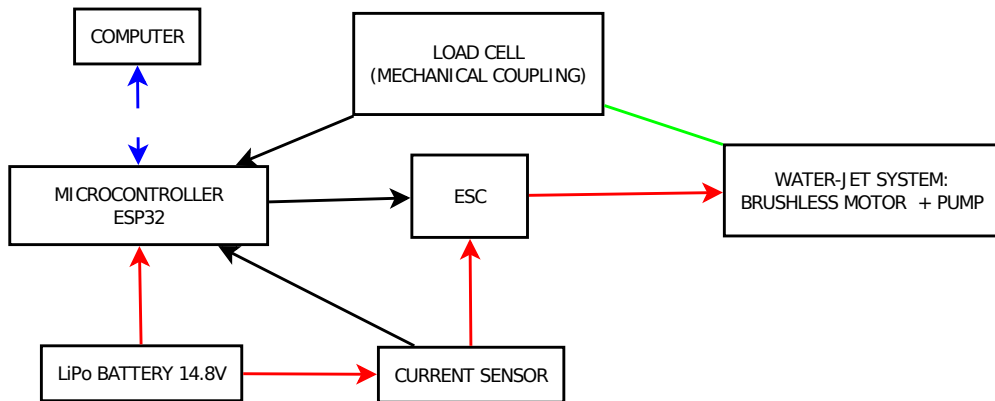


Figure 5.12: Experiment wiring sketch. In Red: power cables; Black: data wiring; Blue: wireless communication; Green: Mechanical coupling.

# 6 Results

Figure 6.1 shows the values of thrust performed by the single-stage old model while Figure 6.2 shows the thrust generated by the two staged proposed designs. As we can see the speed of the boat affects the thrust generated by the water-jet pump. Figure 6.3 show the diagram of velocity in the direction of the axis of the nozzle at the proposed model generated with ANSYS software.

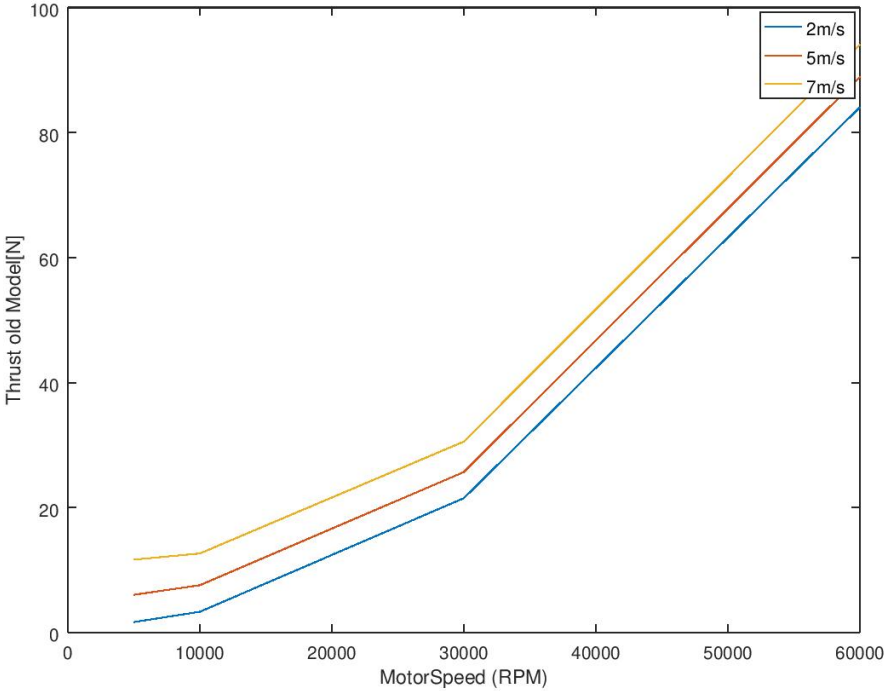


Figure 6.1: Experimental results of the old model.

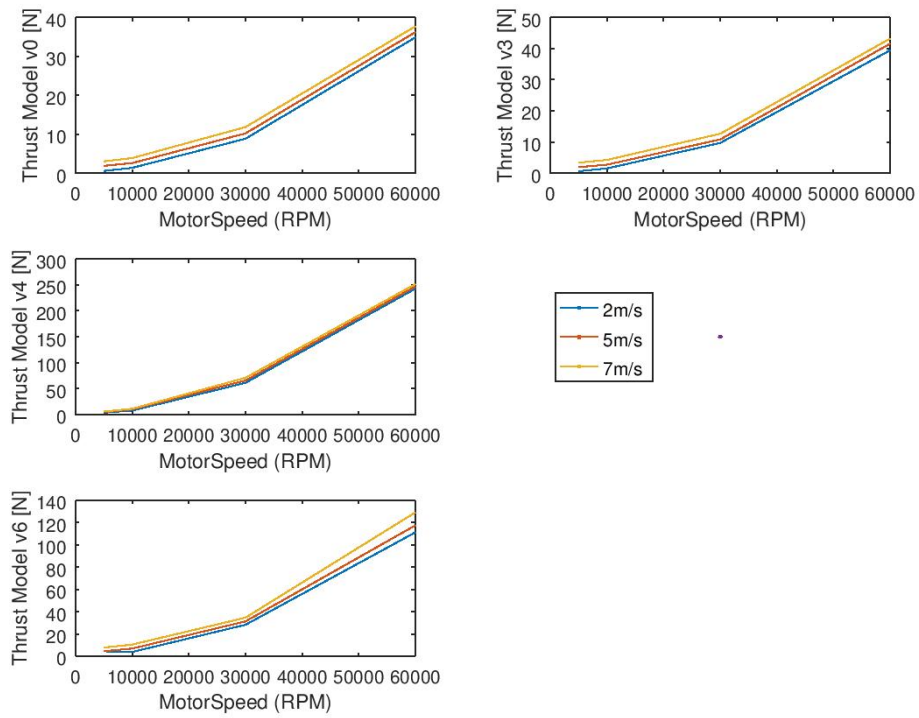


Figure 6.2: Experimental results of the proposed models.

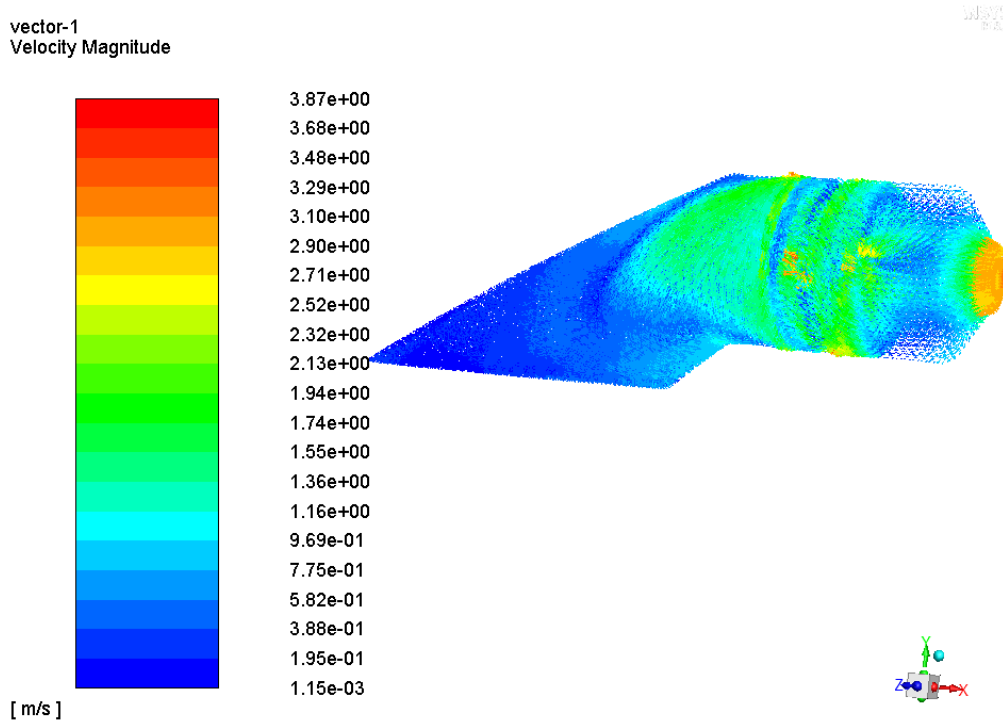


Figure 6.3: Velocity results at the proposed models.

Figure 6.4 and Figure 6.5 show the difference of performance between mathematical model and CFD simulation. There is a big difference between these two curves this is due to the high speed of blades, compressibility of water, friction, turbulence, etc. For having the real values, an experimental analysis must be set in order to obtain the performance considering the efficiency of the brush-less motor. Thrust is calculated as the following equation

$$T = \dot{m} \cdot U_{wj6} \quad (6.1)$$

where  $T[N]$  is the generated thrust,  $\dot{m}[kg/s]$  is mass flow rate and  $U_{wj6}[m/s]$  is the speed of water at the nozzle output[27]. Power of the pump is calculated as:

$$P = 0.5 \cdot \dot{m} \cdot U_{wj6}^2 \quad (6.2)$$

where  $P[W]$  is the power of the pump.

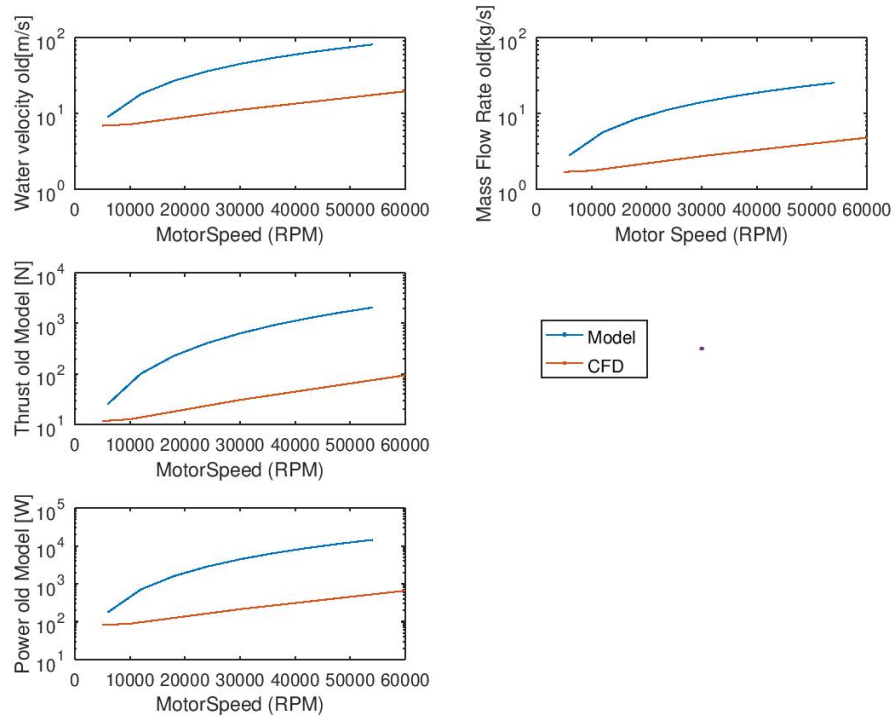


Figure 6.4: Comparison between experimental and theoretical velocity, mass flow rate, thrust and power of the old model @7m/s.

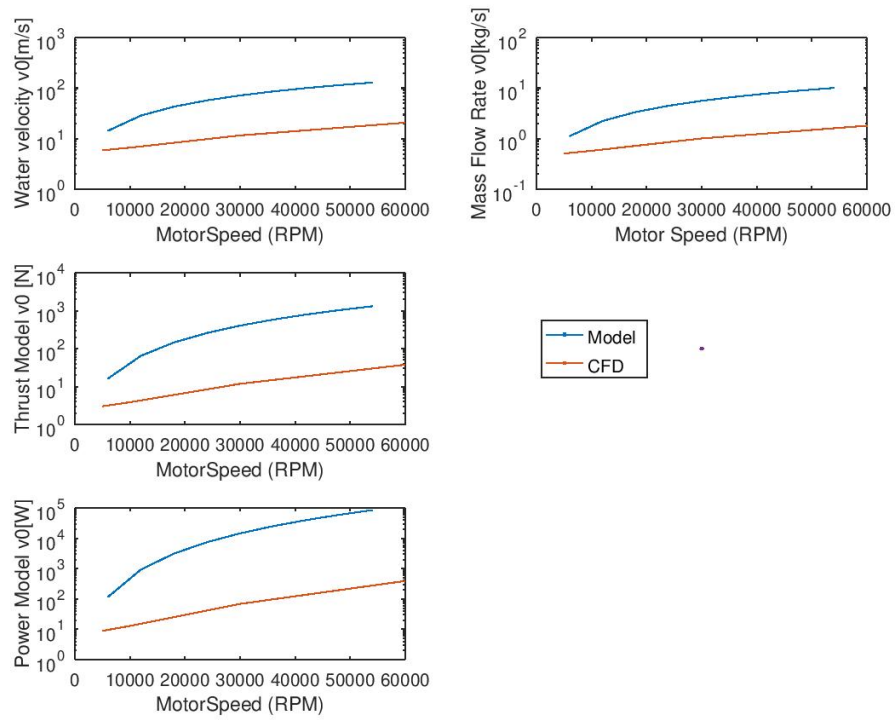


Figure 6.5: Comparison between experimental and theoretical velocity, mass flow rate, thrust and power of the model V0 @7m/s.

## 6.1 Conclusion

In the current Master of Machines and Equipment Design, it is taught theory of fluid mechanics analyzing nozzles and pumps. The thesis goal is to combine that information and apply into a very new field which is using electric motors into high speed water jet propelled boats. Very few information is available locally, therefore after researching using internet two calculation approaches were found: the pump approach, and the water-jet approach. The availability of a model helped to better understand the system as well as see future improvements, such as inlet grid to prevent moisture entering to damage the blade and a thrust vectoring system to allow the ship an omni-directional movement.

Calculation using Octave was not accurate at first due to lack of understanding how to properly calculate flow rate at pump and relate it to thrust. Then after reading NASA rocket thrust theory calculation was improved.

When using CFD numerical simulation, many problems were encountered. At first Ansys software contains it's own blade wizard, which helps to create pumps and turbines very fast and efficiently, however this approach was discarded due to the lack of nozzle coupling.

Second CFD approach consisted in performing simulation of three different parts: Inlet, Blade and Nozzle; as different systems, each system with it's own mesh. However contact between parts was not very accurate, sometimes the parts were isolated one each other, so this approach was also discarded.

Third CFD approach consisted on a full system as a part created in Creo4 and exported as step file to Ansys, where it has to be cutted in order to separate the rotational blades from the static system, as well as perform sweep meshing method were possible. The shaft was deleted in order to get easier simulation. After many attempts most of proposed water jet models had lower thrust than the old model, this was solved after increasing the nozzle diameter.

It is possible to decrease volume of a water-jet pump by adding a second stage of blades, values found in calculation are shown in Table 5.1. The selected model to replace the old one is the model V6 where nozzle and blade diameters had been decreased while increasing the thrust slightly. Increase on NPSH can be solved by limiting the motor speed to by using algorithms of duty cycle control. Materials for blade must be chosen in order to maintain the low price for easy replacement if cavitation damage appear.

Experimental part was not possible to be performed due to the impossibility of access to laboratories for 3D printing and laboratories of fluid mechanics at the faculty.

The results found at Figure 6.4 and Figure 6.5 shown a decrease of efficiency at higher blade speed. It is true that every parameter such as: mass flow rate, outlet velocity  $U_{wj6}$  and power increase with higher mass blade speed. However the relation between theoretical curve and CFD curve increases dramatically due to the high turbulence achieved.

In future projects, it is recommended in order to get better accuracy of results between numerical simulation and model(mathematical calculation), to find a performance equation for thrust according to the blade speed for single stage pump, and two stage pump. These equations can be achieved by processing the experimental data obtained with comparison between numerical simulation and mathematical model. By adding these performance equations to the mathematical calculation it will be possible to have not only more accurate results but also to have a faster comparison between different versions of the proposed water jet pump without spending too much computational time at numerical simulation. It is also necessary to perform an experiment in order to get real values of thrust and find a more accurate equation of performance of whole water jet system.

## Literature

- [1] J. SARAH. “Electric Boats Market Is Booming Worldwide With Strong Growth — Frauscher Boats, LTS Marine, Symphony Boat – Daily Market Insight. DailyMarketInsight.com”. In: *DailyMarketInsight.com* 7 (2019).
- [2] R. ENERGY. “Sweden prepares to launch largest electric car ferry”. In: *Energy Reporters* (2019).
- [3] N. RAMEZ. “How cheap can energy storage get? Very cheap”. In: *Energy Post* (2019).
- [4] I. J. Karassik, J. P. Messina, P. Cooper, and C. C. Herald. “Pump handbook”. In: *McGraw-Hill*. 3 (2001).
- [5] Ittc. “The specialist committee on validation of waterjet test procedures”. In: *Ittc recommended procedures* 24 (2005).
- [6] T. P. ANDERSEN. “Design of Rim Driven Waterjet Pump for Small Rescue Vessel”. In: *Chalmers University of Technology, The Technical University of Denmark* (2014).
- [7] N. Hall. “Vectored Thrust”. In: (2015).
- [8] Y. W. H and Y. A. W. “Handbook of small electric motors”. In: *New York : McGraw-Hill* (2001).
- [9] N. E. M. Association. “NEMA MG 1-2009 Motors and Generators”. In: (2009).
- [10] “Boat Brushless ESC user manual”. In: *ShenZhen, China* ().
- [11] A. JR. and J. D. “Computational Fluid Dynamics”. In: *University of Maryland : McGraw-Hill* (1995).
- [12] J. Murad. “What is  $y^+$  (yplus)?” In: (2018).
- [13] F. R. Menter. “Zonal Two Equation Kappa-Omega Turbulence Models for Aerodynamic Flows”. In: (1993).

- [14] H. K. Versteeg and W. Malalasekera. “An introduction to computational fluid dynamics: The finite volume method”. In: (1995).
- [15] X. Chen and C. Wheeler. “Computational Fluid Dynamics (CFD) modelling of transfer chutes: Assessment of viscosity, drag and turbulence models”. In: (2015).
- [16] T. Carrigan, F. Bagheri, and B. Edge. “The Influence of Meshing Strategies on Simulation Efficiency”. In: (2020).
- [17] Openfoam.com. “OpenFOAM - Official home of The Open Source Computational Fluid Dynamics (CFD) Toolbox.” In: (2019).
- [18] technologyevaluation.com. “Computational Fluid Dynamics Software Overview”. In: (2019).
- [19] MATLAB. “MATLAB - MathWorks”. In: (2019).
- [20] G. Octave. “GNU Octave”. In: (2019).
- [21] 800loadcel.com. “Load Cell and Strain Gauge Basics — Load Cell Central”. In: (2019).
- [22] A. SEMICONDUCTOR. “HX711 24-Bit Analog-to-Digital Converter (ADC) for Weigh Scales”. In: () .
- [23] A. microsystems. “ACS758xCB Thermally Enhanced, Fully Integrated, Hall-Effect-Based Linear Current Sensor IC with 100 Current Conductor”. In: () .
- [24] S. Augarten. “The Most Widely Used Computer on a Chip: The TMS 1000”. In: (1974).
- [25] E. Systems. “ESP32 Series Datasheet”. In: (2019).
- [26] Libelium. “Over the Air Programming with 802.15.4 and ZigBee – OTA”. In: (2011).
- [27] G. R. Center. “Rocket Thrust Equation”. In: (2020).

# Attachments

## A1. Octave function code for calculation of Water-jet parameters

```
1 function [An, BladeVolume, Flow, DynamicPressure,
    Thrust, CTN, JetEfficiencyIdeal, NVR, cm6,
    pressureHead, headCoefficient, specificFlow, SpecificSpeed,
    NPSH, CavitationCoefficient, Uwj6, MassFlowRate] =
    WaterJetEquationsFunctionsv2 (NozzleDiameter, MotorSpeed,
    BladeDiameter, BladeStep, WaterDensity, g, Uwj0)
2 An=pi.*NozzleDiameter.^2./4;
3
4 printf('Water Jet Calculation');
5 RpmToRps=60.0;
6 %WaterSpeed=MotorSpeed./60;
7 %WaterSpeed=[WaterSpeed;2.*WaterSpeed];
8 BladeVolume=(BladeDiameter.^2./4.*pi.*BladeStep);
9 Flow=(MotorSpeed./RpmToRps).*BladeVolume;
10 DynamicPressure=0.5.*(MotorSpeed./RpmToRps.*BladeStep).^2.*
    WaterDensity;
11 %Thrust=WaterDensity.*Flow.*(MotorSpeed./RpmToRps).*
    BladeStep;
12 Uwj6=Flow./An;
13 MassFlowRate=WaterDensity.*Flow;
14 Thrust=MassFlowRate.*Uwj6;
15 CTN=Thrust./(0.5.*WaterDensity.*Uwj0^2.*(An));
16 JetEfficiencyIdeal=4./(3+(1+2.*CTN).^0.5);
```

```

17 NVR=2./JetEfficiencyIdeal -1;
18 cm6=Thrust./(WaterDensity.*Flow).*(An);
19
20 printf('Pump Calculation')
21 pressureHead=0.5.*(MotorSpeed./RpmToRps).^2;
22 headCoefficient=g.*pressureHead./(MotorSpeed./RpmToRps.*
    BladeDiameter/2).^2;
23 specificFlow=Flow./MotorSpeed./RpmToRps./(BladeDiameter/2)
    .^3;
24 SpecificSpeed=MotorSpeed./RpmToRps.*Flow.^0.5./(g.*
    pressureHead.^(3/4));
25 NPSH=(MotorSpeed./RpmToRps).^(4/3).*Flow.^(2/3)./(g.*
    SpecificSpeed.^(4/3));
26 CavitationCoefficient=2.*g.*NPSH./(MotorSpeed./RpmToRps.*
    BladeDiameter/2).^2;
27 endfunction

```

## A2. Octave code for calculation of Water-jet parameters and electric motor parameters, comparing two models

```
1  clc
2  clear all
3  close all
4
5  kv=3650
6  Uwj0=7; %Assuming 1m/s speed
7  dutyCycle=linspace(0,1,10);
8  Voltage=14.8
9  g=9.81
10 MotorSpeed=kv*Voltage.*dutyCycle;
11
12 BladeDiameter=[0.030;0.030];
13 BladeStep=[0.04;0.08];
14 WaterDensity=997
15 NozzleDiameter=[0.02;0.02];
16
17 versions=[4,0];
18
19 for i=versions
20     BladeDiameter
21     NozzleDiameter
22     %An=pi.*NozzleDiameter.^2./4
23
24 [An, BladeVolume, Flow, DynamicPressure, Thrust, CTN,
    JetEfficiencyIdeal, NVR, cm6, pressureHead,
    headCoefficient, specificFlow, SpecificSpeed, NPSH,
    CavitationCoefficient, Uwj6, MassFlowRate] =
    WaterJetEquationsFunctionsV2 (NozzleDiameter, MotorSpeed,
    BladeDiameter, BladeStep, WaterDensity, g, Uwj0);
```

```

25
26
27
28 printf('proposed model Calculations')
29 BladeDiameter(2)=0.025
30 NozzleDiameter(2)=0.01
31 BladeStep(2)=0.023
32 %NozzleDiameter(2)=0.03;
33
34 printf('Figures')
35 hf1 = figure(1)
36 plot(dutyCycle, MotorSpeed)
37 xlabel('Electric Motor Duty Cycle')
38 ylabel('Motor Speed (RPM)')
39 title(strcat('Theoretical performance for:', num2str(kv), 'KV
    Electric Motor @', num2str(Voltage), 'V'))
40
41 hf2 =figure(2)
42 subplot(3,2,1)
43 plot(MotorSpeed, DynamicPressure)
44 %legend('Model', strcat('Proposed design V', num2str(i)))
45 xlabel('MotorSpeed (RPM)')
46 ylabel('Dynamic Pressure(Pa)')
47 subplot(3,2,2)
48 plot(MotorSpeed, Thrust)
49 %legend('Model', strcat('Proposed design V', num2str(i)))
50 xlabel('MotorSpeed (RPM)')
51 ylabel('Thrust (N)')
52 %subplot(3,2,3)
53 %plot(MotorSpeed, CTN)
54 %legend('Model', strcat('Proposed design V', num2str(i)))
55 %xlabel('MotorSpeed (RPM)')
56 %ylabel('Thust Load Coefficient (CTN)')
57 subplot(3,2,3)
58 plot(MotorSpeed, JetEfficiencyIdeal)

```

```

59 %legend('Model',strcat('Proposed design V',num2str(i)))
60 xlabel('MotorSpeed (RPM)')
61 ylabel('Jet Efficiency(Ideal)')
62 subplot(3,2,5)
63 plot(MotorSpeed,NVR)
64 %legend('Model',strcat('Proposed design V',num2str(i)))
65 xlabel('MotorSpeed (RPM)')
66 ylabel('NVR')
67 subplot(3,2,6)
68 plot(MotorSpeed,cm6)
69 %legend('Model',strcat('Proposed design V',num2str(i)))
70 xlabel('MotorSpeed (RPM)')
71 ylabel('Momentum/velocity coeff (cm6)')
72 subplot(3,2,4)
73 plot(0,0, 0,0, 0,0, 0,0)
74 axis off
75 legend('Model',strcat('Proposed design V',num2str(i)), '
    location','west')
76
77 hf3 = figure(3)
78 subplot(3,2,1)
79 plot(MotorSpeed,headCoefficient)
80 %legend('Model',strcat('Proposed design V',num2str(i)))
81 xlabel('MotorSpeed (RPM)')
82 ylabel('Head Coefficient')
83 subplot(3,2,2)
84 semilogy(MotorSpeed,SpecificSpeed)
85 %legend('Model',strcat('Proposed design V',num2str(i)))
86 xlabel('MotorSpeed (RPM)')
87 ylabel('Specific Speed')
88 subplot(3,2,3)
89 semilogy(MotorSpeed,NPSH)
90 %legend('Model',strcat('Proposed design V',num2str(i)))
91 xlabel('MotorSpeed (RPM)')
92 ylabel('NPSH')

```

```

93 subplot(3,2,5)
94 plot(MotorSpeed,CavitationCoefficient)
95 %legend('Model',strcat('Proposed design V',num2str(i)))
96 xlabel('MotorSpeed (RPM)')
97 ylabel('Cavitation Coefficient')
98 subplot(3,2,4)
99 plot(0,0, 0,0, 0,0, 0,0)
100 axis off
101 legend('Model',strcat('Proposed design V',num2str(i)), '
    location','west')
102
103 printf('saving data')
104 %print(hf1, strcat('WaterJetCalculationMotor',num2str(i),'.
    jpg'));
105 print(hf2, strcat('WaterJetCalculationPerformanceComparison
    ',num2str(i),'.jpg'));
106 print(hf3, strcat('WaterJetCalculationPUMP',num2str(i),'.
    jpg'));
107 endfor
108 %close all;
109
110 % _____
111 % COMPARISON WITH DATA OBTAINED
112 % _____
113 CFD_results_filename='ThesisOutput.csv';
114 [SimulationSpeed,SimulationPressure,v_old,m_old,v_0,m_0,v_3,
    m_3,v_4,m_4,v_6,m_6] = thesis_modelling_pump (
    CFD_results_filename);
115
116 hf4 = figure(4)
117 subplot(3,2,1)
118 plot(SimulationSpeed,v_0.*m_0)
119 %legend('2m/s','5m/s','7m/s')
120 xlabel('MotorSpeed (RPM)')
121 ylabel('Thrust Model v0 [N]')

```

```

122 subplot(3,2,2)
123 plot(SimulationSpeed , v_3.*m_3)
124 %legend('2m/s','5m/s','7m/s')
125 xlabel('MotorSpeed (RPM)')
126 ylabel('Thrust Model v3 [N]')
127 subplot(3,2,3)
128 plot(SimulationSpeed , v_4.*m_4)
129 %legend('2m/s','5m/s','7m/s')
130 xlabel('MotorSpeed (RPM)')
131 ylabel('Thrust Model v4 [N]')
132 subplot(3,2,5)
133 plot(SimulationSpeed , v_6.*m_6)
134 %legend('2m/s','5m/s','7m/s')
135 xlabel('MotorSpeed (RPM)')
136 ylabel('Thrust Model v6 [N]')
137 subplot(3,2,4)
138 plot(0,0, 0,0, 0,0, 0,0)
139 axis off
140 legend('2m/s','5m/s','7m/s','location','west')
141
142 hf5 = figure(5)
143 plot(SimulationSpeed , v_old.*m_old)
144 legend('2m/s','5m/s','7m/s')
145 xlabel('MotorSpeed (RPM)')
146 ylabel('Thrust old Model [N]')
147
148 t_old=v_old.*m_old;
149 t_0=v_0.*m_0;
150
151 hf6= figure(6)
152 subplot(3,2,1)
153 semilogy(MotorSpeed ,Uwj6(1,:) ,SimulationSpeed , v_old(:,3))
154 %legend('Model','CFD')
155 xlabel('MotorSpeed (RPM)')
156 ylabel('Water velocity old [m/s]')

```

```

157 subplot(3,2,2)
158 semilogy(MotorSpeed, MassFlowRate(1,:), SimulationSpeed, m_old
           (:,3))
159 %legend('Model', 'CFD')
160 xlabel('Motor Speed (RPM)')
161 ylabel('Mass Flow Rate old [kg/s]')
162 subplot(3,2,3)
163 semilogy(MotorSpeed, Thrust(1,:), SimulationSpeed, t_old(:,3))
164 %legend('Model', 'CFD')
165 xlabel('MotorSpeed (RPM)')
166 ylabel('Thrust old Model [N]')
167 subplot(3,2,5)
168 semilogy(MotorSpeed, Thrust(1,:).*Uwj0, SimulationSpeed, t_old
           (:,3).*Uwj0)
169 %legend('Model', 'CFD')
170 xlabel('MotorSpeed (RPM)')
171 ylabel('Power old Model [W]')
172 subplot(3,2,4)
173 plot(0,0, 0,0, 0,0, 0,0)
174 axis off
175 legend('Model', 'CFD', 'location', 'west')
176
177 hf7= figure(7)
178 subplot(3,2,1)
179 semilogy(MotorSpeed, Uwj6(2,:), SimulationSpeed, v_0(:,3))
180 %legend('Model', 'CFD')
181 xlabel('MotorSpeed (RPM)')
182 ylabel('Water velocity v0 [m/s]')
183 subplot(3,2,2)
184 semilogy(MotorSpeed, MassFlowRate(2,:), SimulationSpeed, m_0
           (:,3))
185 %legend('Model', 'CFD')
186 xlabel('Motor Speed (RPM)')
187 ylabel('Mass Flow Rate v0 [kg/s]')
188 subplot(3,2,3)

```

```

189 semilogy(MotorSpeed, Thrust(2,:), SimulationSpeed, t_0(:,3))
190 %legend('Model', 'CFD')
191 xlabel('MotorSpeed (RPM)')
192 ylabel('Thrust Model v0 [N]')
193 subplot(3,2,5)
194 semilogy(MotorSpeed, Thrust(2,:) .* Uwj6(2,:) .* 0.5,
           SimulationSpeed, t_0(:,3) .* v_0(:,3) .* 0.5)
195 %legend('Model', 'CFD')
196 xlabel('MotorSpeed (RPM)')
197 ylabel('Power Model v0 [W]')
198 subplot(3,2,4)
199 plot(0,0, 0,0, 0,0, 0,0)
200 axis off
201 legend('Model', 'CFD', 'location', 'west')
202
203
204 print(hf4, strcat('ExperimentalResults.jpg'));
205 print(hf5, strcat('ExperimentalResultsOldModel.jpg'));
206 print(hf6, strcat('
           ExperimentalCalculationComparison_OldModel.jpg'));
207 print(hf7, strcat('ExperimentalCalculationComparison_V0.jpg
           '));
208
209 close all;

```

### A3. Octave code for calculation of Water-jet parameters making 3D plots for comparison of nozzle and blade step

```
1  clc
2  clear all
3  close all
4
5  kv=3650
6  Uwj0=7; %Assuming 1m/s speed
7  dutyCycle=linspace(0,1);
8  Voltage=14.8
9  g=9.81
10 %MotorSpeed=2.*kv.*Voltage.*dutyCycle;
11 MotorSpeed=5000;
12
13 BladeDiameterInitial=0.03;
14 BladeStepInitial=0.04;
15 NozzleDiameterInitial=0.02;
16
17 BladeDiameter0=linspace(0.01,BladeDiameterInitial,35);
18 NozzleDiameter0=linspace(0.005,BladeDiameterInitial,4);
19 NozzleDiameter0diff=linspace(0.005,BladeDiameterInitial,3);
20 [BladeDiameter, NozzleDiameter] = meshgrid (BladeDiameter0,
        NozzleDiameter0);
21 %BladeStep=((BladeDiameterInitial.^2.*BladeStepInitial)./(
        BladeDiameter.^2.*2));
22 BladeStep=((BladeDiameterInitial.^2.*BladeStepInitial)./(
        BladeDiameter.^2.*2)).*NozzleDiameter0'./
        NozzleDiameterInitial;
23 WaterDensity=997
24 %NozzleDiameter=0.02
```

```

25 [An, BladeVolume, Flow, DynamicPressure, Thrust, CTN,
    JetEfficiencyIdeal, NVR, cm6, pressureHead,
    headCoefficient, specificFlow, SpecificSpeed, NPSH,
    CavitationCoefficient, Uwj6, MassFlowRate] =
    WaterJetEquationsFunctionsV2 (NozzleDiameter, MotorSpeed,
    BladeDiameter, BladeStep, WaterDensity, g, Uwj0);
26
27 printf('Figures')
28 hf1 = figure(1)
29 plot(BladeDiameter0.*1000, BladeStep.*1000)
30 legend(cellstr(num2str((NozzleDiameter0.*1000)', 'Nozzle=%-
    dmm'))))
31 xlabel('Blade Diameter [mm]')
32 ylabel('Blade Step [mm]')
33 title('Relation between blade diameter and blade step for
    constant Thrust')
34
35 hf2 =figure(2)
36 mesh (BladeDiameter0.*1000, NozzleDiameter0.*1000,
    JetEfficiencyIdeal);
37 xlabel ("Blade Diameter [mm]");
38 ylabel ("Nozzle Diameter [mm]");
39 zlabel ("Ideal Jet Efficiency");
40 title ("Size effect in Efficiency");
41
42 DynamicPressure=DynamicPressure.*(Thrust.*0.+1);
43
44 hf3 =figure(3)
45 subplot(3,2,1)
46 mesh (BladeDiameter0.*1000, NozzleDiameter0.*1000,
    DynamicPressure);
47 xlabel ("Blade [mm]");
48 ylabel ("Nozzle [mm]");
49 zlabel ('Dynamic Pressure [Pa]')
50 subplot(3,2,2)

```

```

51 mesh (BladeDiameter0.*1000, NozzleDiameter0.*1000, Thrust);
52 xlabel ("Blade [mm]");
53 ylabel ("Nozzle [mm]");
54 zlabel ("Thrust [N]");
55 subplot(3,2,3)
56 mesh (BladeDiameter0.*1000, NozzleDiameter0.*1000, CTN);
57 xlabel ("Blade [mm]");
58 ylabel ("Nozzle [mm]");
59 zlabel('CTN')
60 subplot(3,2,4)
61 mesh (BladeDiameter0.*1000, NozzleDiameter0.*1000,
        JetEfficiencyIdeal);
62 xlabel ("Blade [mm]");
63 ylabel ("Nozzle [mm]");
64 zlabel('Jet Efficiency(Ideal)')
65 subplot(3,2,5)
66 %plot(MotorSpeed,NVR)
67 mesh (BladeDiameter0.*1000, NozzleDiameter0.*1000, NVR);
68 xlabel ("Blade [mm]");
69 ylabel ("Nozzle [mm]");
70 zlabel('NVR')
71 subplot(3,2,6)
72 %plot(MotorSpeed,cm6)
73 mesh (BladeDiameter0.*1000, NozzleDiameter0.*1000, cm6);
74 xlabel ("Blade [mm]");
75 ylabel ("Nozzle [mm]");
76 zlabel('cm6')
77
78 hf4 = figure(4)
79 subplot(2,2,1)
80 %plot(MotorSpeed,headCoefficient)
81 mesh (BladeDiameter0.*1000, NozzleDiameter0.*1000,
        headCoefficient);
82 xlabel ("Blade [mm]");
83 ylabel ("Nozzle [mm]");

```

```

84 xlabel('Head Coefficient')
85 subplot(2,2,2)
86 mesh (BladeDiameter0.*1000, NozzleDiameter0.*1000,
        SpecificSpeed);
87 xlabel ("Blade [mm]");
88 ylabel ("Nozzle [mm]");
89 xlabel('Specific Speed')
90 subplot(2,2,3)
91 mesh (BladeDiameter0.*1000, NozzleDiameter0.*1000, NPSH);
92 xlabel ("Blade [mm]");
93 ylabel ("Nozzle [mm]");
94 xlabel('NPSH')
95 subplot(2,2,4)
96 mesh (BladeDiameter0.*1000, NozzleDiameter0.*1000,
        CavitationCoefficient);
97 xlabel ("Blade [mm]");
98 ylabel ("Nozzle [mm]");
99 xlabel('Cavitation Coefficient')
100
101 hf5 =figure(5)
102 subplot(3,2,1)
103 plot ( BladeDiameter0.*1000, DynamicPressure);
104 xlabel ("Blade [mm]");
105 %xlabel ("Nozzle [mm]");
106 ylabel('Dynamic Pressure [Pa]')
107 %legend(strsplit(num2str(BladeDiameter0.*1000)))
108
109 subplot(3,2,2)
110 plot (NozzleDiameter0.*1000, Thrust);
111 %xlabel ("Blade [mm]");
112 xlabel ("Nozzle [mm]");
113 ylabel ("Thrust [N]");
114 %legend(strsplit(num2str(BladeDiameter0.*1000)))
115
116 subplot(3,2,3)

```

```

117 %plot ( NozzleDiameter0.*1000, CTN);
118 %xlabel (" Nozzle [mm]");
119 %ylabel('CTN')
120
121 %subplot(3,2,4)
122 plot (NozzleDiameter0.*1000, JetEfficiencyIdeal);
123 %xlabel (" Blade [mm]");
124 xlabel (" Nozzle [mm]");
125 ylabel('Jet Efficiency(Ideal)')
126 %legend(strsplit(num2str(BladeDiameter0.*1000)))
127
128 subplot(3,2,5)
129 %plot(MotorSpeed,NVR)
130 plot ( NozzleDiameter0.*1000, NVR);
131 %xlabel (" Blade [mm]");
132 xlabel (" Nozzle [mm]");
133 ylabel('NVR')
134 %legend(strsplit(num2str(BladeDiameter0.*1000)))
135
136 subplot(3,2,6)
137 %plot(MotorSpeed,cm6)
138 plot (NozzleDiameter0.*1000, cm6);
139 %xlabel (" Blade [mm]");
140 xlabel (" Nozzle [mm]");
141 ylabel('cm6')
142 %legend(strsplit(num2str(BladeDiameter0.*1000)))
143
144 subplot(3,2,4)
145 plot(0,0, 0,0, 0,0, 0,0)
146 axis off
147 h=legend(cellstr(num2str((NozzleDiameter0.*1000)'),'Nozzle
    =%dmm')), 'location','west')
148 %set (h, " fontsize", 7);
149
150

```

```

151 hf6 = figure(6)
152 subplot(3,2,1)
153 %plot(MotorSpeed, headCoefficient)
154 plot (BladeDiameter0.*1000, headCoefficient);
155 xlabel ("Blade [mm]");
156 %ylabel ("Nozzle [mm]");
157 ylabel('Head Coefficient')
158 subplot(3,2,2)
159 plot (BladeDiameter0.*1000, SpecificSpeed);
160 %legend( cellstr(num2str((NozzleDiameter0.*1000)', 'Nozzle=%-
      dmm')))
161 xlabel ("Blade [mm]");
162 %ylabel ("Nozzle [mm]");
163 ylabel('Specific Speed')
164 subplot(3,2,3)
165 plot (BladeDiameter0.*1000, NPSH);
166 xlabel ("Blade [mm]");
167 %ylabel ("Nozzle [mm]");
168 ylabel('NPSH')
169 subplot(3,2,5)
170 plot (BladeDiameter0.*1000, CavitationCoefficient);
171 xlabel ("Blade [mm]");
172 %ylabel ("Nozzle [mm]");
173 ylabel('Cavitation Coeff')
174 subplot(3,2,4)
175 plot(0,0, 0,0, 0,0, 0,0)
176 axis off
177 legend( cellstr(num2str((NozzleDiameter0.*1000)', 'Nozzle=%-
      dmm')), 'location', 'west')
178 %legend('Model', 'CFD', 'location', 'west')
179
180 %hf7 =figure(7)
181 %plot (NozzleDiameter0diff.*1000, diff(JetEfficiencyIdeal));
182 %xlabel ("Blade [mm]");
183 %xlabel ("Nozzle [mm]");

```

```

184 ylabel('DIFF Jet Efficiency(Ideal)')
185 legend(strsplit(num2str(BladeDiameter0.*1000)))
186
187 i=0;
188 printf('saving data')
189 print(hf1, strcat('WaterJetCalculationBladeStep-Diameter',
    num2str(i),'.jpg'));
190 %print(hf2, strcat('WaterJetCalculationSizeEffect3D',
    num2str(i),'.jpg'));
191 print(hf3, strcat('
    WaterJetCalculationPerformanceComparison3D',num2str(i),'.
    jpg'));
192 print(hf4, strcat('WaterJetCalculationPUMP3D',num2str(i),'.
    jpg'));
193
194 print(hf5, strcat('
    WaterJetCalculationPerformanceComparison2D',num2str(i),'.
    jpg'));
195 print(hf6, strcat('WaterJetCalculationPUMP2D',num2str(i),'.
    jpg'));
196
197 %print(hf7, strcat('WaterJetCalculationDIFFjetEff',num2str(
    i),'.jpg'));
198
199 close all
200
201 % CHOOSING BLADE STEP
202 printf('CHOOSING BLADE STEP')
203 BladeDiameterNew=0.025
204 BladeStepNew=(BladeDiameterInitial^2*BladeStepInitial/2)./
    BladeDiameterNew.^2

```